

MULTIPLE ANTENNA WIRELESS SYSTEMS AND CHANNEL STATE INFORMATION

BY DRAGAN SAMARDZIJA

A dissertation submitted to the
Graduate School—New Brunswick
Rutgers, The State University of New Jersey
in partial fulfillment of the requirements

for the degree of

Doctor of Philosophy

Graduate Program in Electrical and Computer Engineering

Written under the direction of
Professor Narayan B. Mandayam
and approved by

Professor Narayan B. Mandayam

Professor Roy D. Yates

Doctor Larry J. Greenstein

Doctor Gerard J. Foschini

New Brunswick, New Jersey

May, 2004

© 2004

Dragan Samardzija

ALL RIGHTS RESERVED

ABSTRACT OF THE DISSERTATION

Multiple Antenna Wireless Systems and Channel State Information

by Dragan Samardzija

Dissertation Director: Professor Narayan B. Mandayam

The use of multiple antennas in wireless systems have been shown to provide tremendous capacity gains. A key factor in realizing such gains is the knowledge of the channel state information (CSI) at the receiver and transceiver. In this thesis we study the fundamental limits of multiple antenna multiuser systems in the following contexts: (1) pilot-assisted channel state estimation, (2) transmitter optimization with delayed CSI and (3) CSI feedback schemes.

We first analyze the effects of pilot assisted MIMO channel estimation on achievable data rates (lower bound on information capacity) over a frequency flat time-varying channel. Under a block-fading channel model, the effects of the estimation error are evaluated in the case of the estimates being available at the receiver only (open loop), and in the case when the estimates are fed back to the transmitter allowing water pouring transmitter optimization (closed loop). Using a characterization of the effective noise due to estimation error, we analyze the achievable rates as a function of the power allocated to the pilot, the channel coherence time, the background noise level as well as the number of transmit and receive antennas. We observe that as the number of transmit antennas increases, the sensitivity to the channel response estimation error is more pronounced (while keeping the same number of receive antennas). It is also seen that in certain cases, it is better to use the open loop scheme as opposed to the closed loop scheme. The analysis presented here can be used to optimally allocate pilot power for various system and channel operating conditions, and also to determine the effectiveness of closed loop feedback.

Next, we consider multiple antenna transmitter optimization schemes that are based on

linear transformations and transmit power optimization, while keeping the average transmit power conserved. We consider the downlink of a wireless system with multiple transmit antennas at the base station and a number of mobile terminals (i.e., users) each with a single receive antenna. We consider the maximum achievable sum data rates in the case of (1) zero-forcing spatial pre-filter, (2) modified zero-forcing spatial pre-filter and (3) triangularization spatial pre-filtering coupled with dirty paper coding transmission scheme. Using a multiple input single output (MISO) channel model with temporal and spatial correlations, we study the effect of delayed CSI on these schemes. It is seen that as the CSI delay increases, spatially uncorrelated channels perform worse than spatially correlated channels, which is in contrast to the case of zero delay CSI. A linear minimum mean squared error (MMSE) predictor of the channel state is introduced which can improve the performance in all cases. Further, the predictor increases the tolerable maximum CSI delay for which the performance on spatially uncorrelated channels is higher than that of the correlated case.

Finally, we propose a CSI feedback scheme based on unquantized and uncoded (UQ-UC) transmission. We consider a system where a mobile terminal obtains the downlink CSI and feeds it back to the base station using an uplink feedback channel. If the downlink channel is an independent Rayleigh fading channel, then the CSI may be viewed as an output of a complex independent identically distributed Gaussian source. Further, if the uplink feedback channel is AWGN, it can be shown that that UQ-UC CSI transmission (that incurs zero delay) is optimal in that it achieves the same MMSE distortion as a scheme that optimally (in the Shannon sense) quantizes and encodes the CSI while theoretically incurring infinite delay. Since the UQ-UC transmission is suboptimal on correlated wireless channels, we propose a simple linear CSI feedback receiver that can be used to improve the performance of UQ-UC transmission while still retaining the attractive zero-delay feature. We provide bounds on the performance of the UQ-UC CSI feedback and also explore the performance in multiple antenna multiuser wireless systems.

Table of Contents

Abstract	ii
List of Figures	vi
1. Introduction	1
2. Pilot Assisted Estimation of MIMO Fading Channel Response and Achievable Data Rates	4
2.1. System Model	5
2.2. Estimation of Channel Response	9
2.3. Estimates Available to Receiver:	
Open Loop Capacity	11
2.4. Estimates Available to Transmitter and Receiver:	
Closed Loop Capacity	13
2.5. Examples and Numerical Results	15
2.5.1. SISO Systems	15
2.5.2. MIMO Systems	16
2.6. Conclusion	21
3. Downlink Multiple Antenna Transmitter Optimization on Spatially and Temporally Correlated Channels with Delayed Channel State Information	23
3.1. System Model and Transmitter Optimization Schemes	24
3.2. Channel Model	32
3.3. Channel State Prediction	40
3.4. Conclusion	44

4. Unquantized and Uncoded Channel State Information Feedback on Wireless Channels	45
4.1. Background	45
4.2. UQ-UC CSI Feedback	47
4.3. UQ-UC CSI Feedback on Correlated Channels	48
4.3.1. Performance Bounds	50
4.3.2. Feedback Receivers for Enhancing UQ-UC CSI Feedback Schemes	51
4.3.3. Numerical Results: Distortion Performance	53
4.4. Case Study: UQ-UC CSI Feedback for Transmitter Optimization in Mul- tiple Antenna Multiuser Systems	55
4.4.1. Numerical Results: Information Rates in Multiuser Systems . . .	57
4.5. Conclusion	58
5. Conclusion	60
5.1. Future Directions	62
Appendix A. Virtual Uplink and Proof of Proposition 2	64
Appendix B. Dirty Paper Coding	66
Appendix C. ARMA Model and Approximation of the Jakes Model .	68
References	70
Vita	76

List of Figures

2.1.	Achievable open loop rates vs. power allocated to the pilot, SISO system, $SNR = 4, 12, 20\text{dB}$, coherence time $K = 10$, Rayleigh channel.	16
2.2.	Capacity efficiency ratio vs. channel coherence time ($K = 10, 20, 40, 100$), SISO system, $SNR = 4, 20\text{dB}$, Rayleigh channel.	17
2.3.	Achievable open loop rates vs. power allocated to the pilot, MIMO system, $SNR = 12\text{dB}$, coherence time $K = 40$, Rayleigh channel, solid line corresponds to a system with the channel response estimation, and dashed line to the case of the ideal channel response knowledge.	18
2.4.	Capacity efficiency ratio vs. channel coherence time ($K = 10, 20, 40, 100$), MIMO system, $SNR = 12\text{dB}$, Rayleigh channel.	18
2.5.	Ergodic capacity vs. SNR, MIMO system, ideal knowledge of the channel response, Rayleigh channel, solid line corresponds to open loop capacity, and dashed line to closed loop capacity (perfect temporal match $\mathbf{H}_{i-1} = \mathbf{H}_i$ is assumed).	19
2.6.	CDF of capacity, MIMO system, $SNR = 4\text{dB}$, ideal knowledge of the channel response, Rayleigh channel, solid line corresponds to open loop capacity, and dashed line to closed loop capacity (perfect temporal match $\mathbf{H}_{i-1} = \mathbf{H}_i$ is assumed).	20
2.7.	Achievable closed loop rates vs. correlation between successive channel responses, MIMO system, $SNR = 4\text{dB}$, coherence time $K = 40$, Rayleigh channel, solid line corresponds to a system with the channel response estimation, and dashed line to the case of the ideal channel response available at the transmitter and the receiver (but with the temporal mismatched $\mathbf{H}_{i-1} \neq \mathbf{H}_i$).	21

2.8.	Achievable closed loop and open loop rates vs. correlation between successive channel responses, MIMO system 4×4 , $SNR = 4\text{dB}$, coherence time $K = 40$, Rayleigh channel, solid line corresponds to a system with the channel response estimation, and dashed line to the case of the ideal channel response available at the transmitter and the receiver (but with the temporal mismatched $\mathbf{H}_{i-1} \neq \mathbf{H}_i$).	22
3.1.	System model consisting of M transmit antennas and N mobile terminals. . .	24
3.2.	Average rate per user vs. SNR, $M = 3$, $N = 3$, Rayleigh channel.	30
3.3.	CDF of rates, $SNR = 10\text{dB}$, per user, $M = 3$, $N = 3$, Rayleigh channel. . . .	31
3.4.	Average rate per user vs. M/N , $SNR = 10\text{dB}$, $N = 3$, variable number of transmit antenna $M = 3, 6, 12, 24$, Rayleigh channel.	31
3.5.	Average rate per user vs. temporal channel correlation k , $SNR = 10\text{dB}$, $M = 3$ (solid lines), $M = 6$ (dashed lines), $N = 3$, Rayleigh channel.	33
3.6.	$\zeta(t)$ for $M = 3$ and channel based on model in (3.26), $f_c = 2\text{GHz}$, $v = 30\text{kmph}$.	37
3.7.	The ZF scheme, average rate per user vs. CSI delay, $SNR = 10\text{dB}$, $M = 3$, $N = 3$, channel based on model in (3.26), $f_c = 2\text{GHz}$, $v = 30\text{kmph}$	38
3.8.	The MZF scheme, average rate per user vs. CSI delay, $SNR = 10\text{dB}$, $M = 3$, $N = 3$, channel based on model in (3.26), $f_c = 2\text{GHz}$, $v = 30\text{kmph}$	38
3.9.	$\rho_n(\tau)$ for $M = 3$, $N = 3$ and channel based on model in (3.26), $f_c = 2\text{GHz}$, $v = 30\text{kmph}$	39
3.10.	Normalized mean squared error between assumed and true channel state vs. CSI delay, with MMSE prediction (dashed lines) and without MMSE prediction (solid lines), $M = 3$, $N = 3$, channel based on model in (3.26), $f_c = 2\text{GHz}$, $v = 30\text{kmph}$	42
3.11.	The ZF scheme, average rate per user vs. CSI delay, with MMSE prediction (dashed lines) and without MMSE prediction (solid lines), $SNR = 10\text{dB}$, $M = 3$, $N = 3$, channel based on model in (3.26), $f_c = 2\text{GHz}$, $v = 30\text{kmph}$	43
3.12.	The MZF scheme, average rate per user vs. CSI delay, with MMSE prediction (dashed lines) and without MMSE prediction (solid lines), $SNR = 10\text{dB}$, $M = 3$, $N = 3$, channel based on model in (3.26), $f_c = 2\text{GHz}$, $v = 30\text{kmph}$	43

4.1.	Unquantized and uncoded transmission that achieves the MMSE distortion of the transmitted signal.	46
4.2.	Communication system with CSI feedback.	48
4.3.	CDMA mobile terminal that applies the UQ-UC CSI feedback.	49
4.4.	MSE vs. CSI update period, $f_c = 2\text{GHz}$, $v = 10\text{kmph}$, average $SNR_{ul}^{csi} = 10\text{dB}$.	54
4.5.	MSE vs. CSI update period, linear receiver, $f_c = 2\text{GHz}$, different mobile terminal velocities 10, 20, 40, 80kmph, average $SNR_{ul}^{csi} = 10\text{dB}$	54
4.6.	System model consisting of M transmit antennas and N mobile terminals. . .	56
4.7.	Average downlink sum data rate vs. the mobile terminal velocity, for CSI update period $\tau = 2\text{msec}$, $f_c = 2\text{GHz}$, $M = 3$, $N = 3$, spatially uncorrelated, downlink data $SNR_{dl} = 10\text{dB}$ and uplink CSI feedback $SNR_{ul}^{csi} = 10\text{dB}$	58

Chapter 1

Introduction

For several emerging wireless data services, the application of multiple antenna systems appears to be one of the most promising solutions leading to even higher data rates and/or the ability to support greater number of users. Multiple transmit and multiple receive antenna systems that embody an implementation of the multi-input multi-output (MIMO) concept in wireless systems [1], have been shown to be able to provide the necessary capacity and also flexibility required for supporting a variety of high data rate applications. Theoretical capacity gains in a single-user system that have been shown to scale (approximately) linearly in the number of antennas [1,2], have fueled further studies related to various aspects of MIMO systems: propagation [3–5], detection [6–14], space-time coding and implementation aspects [15–24], to name a few. There have also been a host of considerations for multiple antenna systems with multiple users (see for example, [25–33]).

A key attribute required of any multiple antenna technique is the need for reliable channel state information (CSI). Such CSI is absolutely necessary at the receiver to realize the potential capacity gains. Further, the CSI is also necessary at the transmitter in the case of transmitter optimization techniques used in conjunction with multiple antennas.

The challenges in estimating CSI in MIMO systems (compared to single-input single-output (SISO) systems) is not only greater because of the large number of parameters that have to be estimated, but it is further exacerbated by the need to support wider channel bandwidths, mobility and the migration of future wireless data services to higher carrier frequencies. For example, wider channel bandwidths result in greater

frequency selectivity, while using higher carrier frequencies results in more spatial variations of the electro-magnetic field. While the fundamental limits of the performance of multiple antenna systems have been characterized in terms of unreliable and/or absent CSI [34, 35], there have been relatively few efforts in relating such fundamental limits to the specifics of signal processing algorithms required for enabling knowledge of CSI. A few efforts in this direction including our own work have been [36–39].

Further, the tremendous capacity gains due to transmitter optimization in multiple antenna multiuser wireless systems [25–27, 32, 33, 40] rely heavily on the availability of the CSI at the transmitter. In such scenarios, aside from the issue of how to estimate the CSI, another interesting question is how to transmit (or feedback) the CSI? For example, what are the most efficient ways of transmitting the CSI back to the transmitter for the purposes of transmitter optimization? These are just a few motivations for studying the implications of channel variations on achievable data rates in wireless systems.

In Chapter 2 we analyze the effects of pilot assisted MIMO channel estimation on achievable data rates (lower bound on information capacity) over a frequency flat time-varying channel [39, 41]. Under a block-fading channel model, the effects of the estimation error are evaluated in the case of the estimates being available at the receiver only (open loop), and in the case when the estimates are fed back to the transmitter allowing water pouring transmitter optimization (closed loop). Using a characterization of the effective noise due to estimation error, we analyze the achievable rates as a function of the power allocated to the pilot, the channel coherence time, the background noise level as well as the number of transmit and receive antennas. We observe that as the number of transmit antennas increases, the sensitivity to the channel response estimation error is more pronounced (while keeping the same number of receive antennas). It is also seen that in certain cases, it is better to use the open loop scheme as opposed to the closed loop scheme. The analysis presented here can be used to optimally allocate pilot power for various system and channel operating conditions, and also to determine the effectiveness of closed loop feedback.

In Chapter 3 we consider multiple antenna transmitter optimization schemes that are based on linear transformations and transmit power optimization, while keeping

the average transmit power conserved. We consider the downlink of a wireless system with multiple transmit antennas at the base station and a number of mobile terminals (i.e., users) each with a single receive antenna. We consider the maximum achievable sum data rates in the case of (1) zero-forcing spatial pre-filter, (2) modified zero-forcing spatial pre-filter and (3) triangularization spatial pre-filtering coupled with dirty paper coding transmission scheme. Using a multiple input single output (MISO) channel model with temporal and spatial correlations, we study the effect of delayed CSI on these schemes. It is seen that as the CSI delay increases, spatially uncorrelated channels perform worse than spatially correlated channels, which is in contrast to the case of zero delay CSI. A linear minimum mean squared error (MMSE) predictor of the channel state is introduced which can improve the performance in all cases. Further, the predictor increases the tolerable maximum CSI delay for which the performance on spatially uncorrelated channels is higher than that of the correlated case.

Finally in Chapter 4 we propose a CSI feedback scheme based on unquantized and uncoded (UQ-UC) transmission [42]. We consider a system where a mobile terminal obtains the downlink CSI and feeds it back to the base station using an uplink feedback channel. If the downlink channel is an independent Rayleigh fading channel, then the CSI may be viewed as an output of a complex independent identically distributed Gaussian source. Further, if the uplink feedback channel is AWGN, it can be shown that that UQ-UC CSI transmission (that incurs zero delay) is optimal in that it achieves the same MMSE distortion as a scheme that optimally (in the Shannon sense) quantizes and encodes the CSI while theoretically incurring infinite delay. Since the UQ-UC transmission is suboptimal on correlated wireless channels, we propose a simple linear CSI feedback receiver that can be used to improve the performance of UQ-UC transmission while still retaining the attractive zero-delay feature. We provide bounds on the performance of the UQ-UC CSI feedback and also explore the performance in multiple antenna multiuser wireless systems.

We conclude in Chapter 5.

Chapter 2

Pilot Assisted Estimation of MIMO Fading Channel Response and Achievable Data Rates

In this chapter we analyze how the estimation error of the channel response affects the performance of a MIMO wireless system. Considering the practical importance of SISO systems, we analyze them as a subset of MIMO systems. Following terminology in the literature (see [43] and references therein), the channel response estimate is termed CSI. We assume a frequency-flat time-varying wireless channel with additive white Gaussian noise (AWGN). More precisely, a quasi-static block-fading channel model is used. Furthermore, the temporal variations of the channel are characterized by the correlation between successive channel blocks. The above system may also correspond to one subchannel (i.e., carrier) of an OFDM wireless system [44]. We consider two pilot (training) arrangement schemes in this study. The first scheme uses a single pilot symbol per block with different power than the data symbol power. The second scheme uses more than one pilot symbol per block, whose power is the same as the data symbol power. For the given pilot schemes, in both cases, *maximum-likelihood* (ML) estimation of the channel response is considered [45]. In the MIMO case, orthogonality between the pilots assigned to different transmit antennas is assumed. The effects of the estimation error are evaluated in the case of the estimates being available at the receiver only, and in the case when the estimates are fed back to the transmitter allowing water pouring optimization. The presented analysis may be viewed as a study of mismatched receiver and transmitter algorithms in MIMO systems. The analysis connects results of information theory (see [34, 35] and references therein) with practical wireless communication systems (employing pilot assisted channel estimation) and

generalizing it to MIMO systems. Previously published studies on MIMO channel estimation and its effects include [36] and [37]. An elaborate information theoretic study analyzing different training schemes, and optimizing their parameters to maximize the open loop MIMO capacity lower bounds, is also presented in [38]. We will highlight the similarities and differences of the work presented here to that in [38] in the subsequent sections. We believe that the results presented here are directly applicable to current and next generation wireless systems [21–23,46]. Furthermore, the results may be used as baseline benchmarks for performance evaluation of more advanced estimation and transmitter optimization schemes, such as anticipated in future systems.

2.1 System Model

In the following we present a MIMO communication system that consists of M transmit and N receive antennas (denoted as a $M \times N$ system). At the receiver we assume sampling with the period $T_{smp} = 1/B$, where B is the signal bandwidth, thus preserving the sufficient statistics. The received signal is a spatial vector \mathbf{y}

$$\mathbf{y}(k) = \mathbf{H}(k)\mathbf{x}(k) + \mathbf{n}(k), \quad \mathbf{y}(k) \in \mathcal{C}^N, \mathbf{x}(k) \in \mathcal{C}^M, \mathbf{n}(k) \in \mathcal{C}^N, \mathbf{H}(k) \in \mathcal{C}^{N \times M} \quad (2.1)$$

where $\mathbf{x}(k) = [g_1(k) \cdots g_M(k)]^T$ is the transmitted vector, $\mathbf{n}(k) = [n_1(k) \cdots n_N(k)]^T$ is the AWGN vector with $(E[\mathbf{n}(k)\mathbf{n}(k)^H] = N_0 \mathbf{I}_{N \times N})$, and $\mathbf{H}(k)$ is the MIMO channel response matrix, all corresponding to the time instance k . We assign index $m = 1, \dots, M$ to denote the transmit antennas, and index $n = 1, \dots, N$ to denote the receive antennas. Thus, $h_{nm}(k)$ is the n th row and m th column element of the matrix $\mathbf{H}(k)$. Note that it corresponds to a SISO channel response between the transmit antenna m and the receive antenna n . $g_m(k)$ is the transmitted signal from the m th transmit antenna. The n th component of the received spatial vector $\mathbf{y}(k) = [y_1(k) \cdots y_N(k)]^T$ (i.e., signal at the receive antenna n) is

$$y_n(k) = \sum_{m=1}^M h_{nm}(k)g_m(k) + n_n(k). \quad (2.2)$$

To perform estimation of the channel response $\mathbf{H}(k)$, the receiver uses a pilot (training) signal that is a part of the transmitted data. The pilot is sent periodically, every K

sample periods. We consider the transmitted signal to be comprised of two parts: one is the data bearing signal and the other is the pilot signal. Within the pilot period consisting of K symbols, L symbols (i.e., signal dimensions) are allocated to the pilot, per transmit antenna. As a common practical solution (see [21–23,47]), we assume that the pilot signals assigned to the different transmit antennas, are mutually orthogonal. For more details on signal design for multiple transmit antenna systems see also [7,48]. This assumption requires that $K \geq LM$. Consequently we define a K -dimensional temporal vector $\mathbf{g}_m = [g_m(1) \cdots g_m(K)]^T$, whose k th component is $g_m(k)$ (in (2.2)), as

$$\mathbf{g}_m = \underbrace{\sum_{i=1}^{K-LM} a_{im}^d d_{im}^d \mathbf{s}_i^d}_{\text{Data}} + \underbrace{\sum_{j=1}^L a_{jm}^p d_{jm}^p \mathbf{s}_{jm}^p}_{\text{Pilot}}. \quad (2.3)$$

In the above the first sum is the information, i.e., data bearing signal and the second corresponds to the pilot signal, corresponding to the transmit antenna m . Superscripts "d" and "p" denote values assigned to the data and pilot, respectively. d_{im}^d is the unit-variance circularly symmetric complex data symbol. The pilot symbols (d_{jm}^p , $j = 1, \dots, L$) are predefined and known at the receiver. Without loss of generality, we assume that $|d_{jm}^p|^2 = 1$. We also assume that the amplitudes are $a_{im}^d = A$, and $a_{jm}^p = A_P$, and they are known at the receiver. Further, the amplitudes are related as $A_P = \alpha A$. Note that the amplitudes are identical across the transmit antennas (because we assumed that the transmit power is equally distributed across them).

Furthermore, $\mathbf{s}_i^d = [s_i^d(1) \cdots s_i^d(K)]^T$ and $\mathbf{s}_{jm}^p = [s_{jm}^p(1) \cdots s_{jm}^p(K)]^T$, ($i = 1, \dots, (K-LM)$, $j = 1, \dots, L$, and $m = 1, \dots, M$) are waveforms, denoted as *temporal signatures*. The temporal signatures are mutually orthogonal. For example, \mathbf{s}_i^d (or \mathbf{s}_{jm}^p) could be a canonical waveform such as a TDMA-like waveform, where \mathbf{s}_i^d (or \mathbf{s}_{jm}^p) is the unit-pulse at the time instance i . Alternately, \mathbf{s}_i^d (or \mathbf{s}_{jm}^p) could also be a K -dimensional CDMA sequence spanning all K sample intervals [46]. Note that the above model while being general enough is particularly suitable for MIMO implementations over CDMA systems (see [47]).

As said earlier, we assume that the pilot signals are orthogonal between the transmit antennas. The indexing and summation limits in (2.3) conform to this assumption, i.e.,

temporal signatures $\mathbf{s}_{jm}^p (j = 1, \dots, L)$ are uniquely assigned to the transmit antenna m . In other words, transmit antenna m must not use the temporal signatures that are assigned as pilots to other antennas and assigned to data, which is consequently lowering the achievable data rates (this will be revisited in the following sections). Unlike the pilot temporal signatures, the data bearing temporal signatures $\mathbf{s}_i^d (i = 1, \dots, (K - LM))$ are reused across the transmit antennas, which is an inherent property of MIMO systems, potentially resulting in high achievable data rates. It is interesting to note that the assumptions regarding the orthogonality between the pilots (motivated by practical considerations) are also shown to be optimal in [38], maximizing the open loop capacity lower bound. Similar conclusions are drawn in [7, 36]. We rewrite the received spatial vector in (2.1) as

$$\mathbf{y}(k) = \mathbf{H}(k)(\mathbf{d}(k) + \mathbf{p}(k)) + \mathbf{n}(k), \quad \mathbf{d}(k) \in \mathcal{C}^M, \mathbf{p}(k) \in \mathcal{C}^M \quad (2.4)$$

where $\mathbf{d}(k)$ is the information, i.e., data bearing signal and $\mathbf{p}(k)$ is the pilot portion of the transmitted spatial signal, at the time instance k . The m th component of the data vector $\mathbf{d}(k) = [d_1(k) \cdots d_M(k)]^T$ (i.e., data signal at the transmit antenna m) is

$$d_m(k) = \sum_{i=1}^{K-LM} a_{im}^d d_{im}^d s_i^d(k). \quad (2.5)$$

The m th component of the pilot vector $\mathbf{p}(k) = [p_1(k) \cdots p_M(k)]^T$ (i.e., pilot signal at the transmit antenna m) is

$$p_m(k) = \sum_{j=1}^L a_{jm}^p d_{jm}^p s_{jm}^p(k). \quad (2.6)$$

Let us now describe the assumed properties of the MIMO channel $\mathbf{H}(k)$. The channel coherence time is assumed to be greater than or equal to KT_{smp} . This assumption approximates the channel to be constant over at least K samples ($h_{nm}(k) \approx h_{nm}$, for $k = 1, \dots, K$, for all m and n), i.e., approximately constant during the pilot period. In the literature, channels with the above property are known as block-fading channels [44]. Furthermore, we assume that the elements of \mathbf{H} are independent identically distributed (*iid*) random variables, corresponding to highly scattering channels. In general, the MIMO propagation measurements and modeling have shown that the elements of \mathbf{H}

are correlated (i.e., not independent) [3–5]. The effects of correlation on the capacity of MIMO systems is studied in [49]. Assuming independence is a common practice because the information about correlation is usually not available at the receiver and/or the correlation is time varying (not stationary) and hard to estimate. Based on the above, the received temporal vector at the receiver n , whose k th component is $y_n(k)$ (in (2.2)), is

$$\mathbf{r}_n = [y_n(1) \cdots y_n(K)]^T = \sum_{m=1}^M h_{nm} \mathbf{g}_m + \mathbf{n}_n, \quad \mathbf{r}_n \in \mathcal{C}^K \quad (2.7)$$

where $\mathbf{n}_n = [n_n(1) \cdots n_n(K)]^T$ and $\mathbb{E}[\mathbf{n}_n \mathbf{n}_n^H] = N_0 \mathbf{I}_{K \times K}$.

Note that when varying the number of transmit antennas, the total average transmitted power must stay the same, i.e., conserved. This is a common assumption in MIMO systems [1, 2]. Also, the power is equally distributed across the transmit antennas. The average transmit power (from all transmit antennas) is

$$P_{av} = M \frac{\left(\sum_{i=1}^{K-LM} (a_{im}^d)^2 + \sum_{j=1}^L (a_{jm}^p)^2 \right)}{K} = M \frac{((K-LM) + L\alpha^2)A^2}{K}. \quad (2.8)$$

Thus

$$A = \sqrt{\frac{K}{((K-LM) + \alpha^2 L)} \frac{P_{av}}{M}}. \quad (2.9)$$

As seen from the above, we assume that the total average transmitted energy (within the pilot period) is the same, but differently distributed between the data bearing portion of the signal and the pilot. Consequently, we observe the performance of the system with respect to the amount of transmitted energy that is allocated to the pilot (percentage wise). This percentage is denoted as μ and is given as

$$\mu = \frac{L\alpha^2}{(K-LM) + L\alpha^2} 100 \text{ [%]}. \quad (2.10)$$

As said earlier, in this study we consider two different pilot arrangements:

1. $L = 1$ and $A_P \neq A$. The amplitude is

$$A_1 = \sqrt{\frac{K}{((K-M) + \alpha^2)} \frac{P_{av}}{M}}. \quad (2.11)$$

In the remainder of the chapter, the above pilot arrangement is referred to as case 1. For example, in SISO systems the above pilot arrangement is applied in

CDMA wireless systems (e.g., IS-95 and WCDMA [46]). In MIMO systems, it is applied in narrowband MIMO implementations described in [21–23]. It is also applied in a wideband MIMO implementation based on 3G WCDMA [47]. Note that under certain assumptions to be pointed out in the next section, the above pilot arrangement scheme is equivalent to the scheme in [38]

2. $L \geq 1$ and $A_P = A$ ($\alpha = 1$). The amplitude is

$$A_2 = \sqrt{\frac{K}{(K - L(M - 1))} \frac{P_{av}}{M}}. \quad (2.12)$$

In the remainder of the chapter, the above pilot arrangement is referred to as case 2. Note that the above pilot arrangement is frequently used in SISO systems, e.g., wire-line modems [50] and some wireless standards (e.g., IS-136 and GSM [44]). This arrangement is typically not used in MIMO systems.

In Section 2.5 we will analyze the performance of these two cases because they are widely applied in different communication systems.

2.2 Estimation of Channel Response

Due to the orthogonality of the pilots and assumption that the elements of \mathbf{H} are *iid*, it can be shown that to obtain the maximum likelihood estimate of \mathbf{H} it is sufficient to estimate h_{nm} (for $m = 1, \dots, M$, $n = 1, \dots, N$), independently¹. This is identical to estimating a SISO channel response between the transmit antenna m and receive antenna n . The estimation is based on averaging the projections of the received signal on $d_{jm}^p \mathbf{s}_{jm}^p$ (for $j = 1, \dots, L$ and $m = 1, \dots, M$) as

$$\begin{aligned} \hat{h}_{nm} &= \frac{1}{LA_P} \sum_{j=1}^L (d_{jm}^p \mathbf{s}_{jm}^p)^H \mathbf{r}_n \\ &= \frac{1}{L} \sum_{j=1}^L (h_{nm} + (d_{jm}^p \mathbf{s}_{jm}^p)^H \mathbf{n}_n / A_P) \end{aligned}$$

¹Based on the above assumptions it can be shown that in this particular case the ML estimate is equal to the LMMSE estimate considered in [38].

$$= h_{nm} + \frac{1}{LA_P} \sum_{j=1}^L (d_{jm}^p \mathbf{s}_{jm}^p)^H \mathbf{n}_n \quad (2.13)$$

where \hat{h}_{nm} denotes the estimate of the channel response h_{nm} . It can be shown that for a frequency-flat AWGN channel, given the pilot signal and the assumed properties of \mathbf{H} , (2.13) is the maximum-likelihood estimate of the channel response h_{nm} [45]. The estimation error is

$$n_{nm}^e = \frac{1}{LA_P} \sum_{j=1}^L (d_{jm}^p \mathbf{s}_{jm}^p)^H \mathbf{n}_n. \quad (2.14)$$

n_{nm}^e corresponds to a Gaussian random variable with distribution $\mathcal{N}_{\mathcal{C}}(0, N_0/(L(\alpha A)^2))$. Thus, the channel matrix estimate $\hat{\mathbf{H}}$ is

$$\hat{\mathbf{H}} = \mathbf{H} + \mathbf{H}_e \quad (2.15)$$

where \mathbf{H}_e is the estimation error. Each component of the error matrix \mathbf{H}_e is an independent and identically distributed random variable n_{nm}^e given in (2.14) (where n_{nm}^e is the n th row and m th column element of \mathbf{H}_e).

Having the channel response estimated, the estimate of the transmitted data that is associated with the temporal signature \mathbf{s}_i^d is obtained starting from the following statistics

$$z_{ni} = \frac{1}{A} (\mathbf{s}_i^d)^H \mathbf{r}_n \quad (2.16)$$

where the amplitude A is assumed to be known at the receiver. z_{ni} corresponds to the n th component of the vector

$$\mathbf{z}_i = [z_{1i} \cdots z_{Ni}]^T = \mathbf{H} \mathbf{d}_i + \frac{1}{A} \mathbf{n}_i, \quad i = 1, \dots, K - LM \quad (2.17)$$

where the m th component of $\mathbf{d}_i = [d_{i1}^d \cdots d_{iM}^d]^T$ is d_{im}^d (data transmitted from the antenna m and assigned to the temporal signature \mathbf{s}_i^d). Further, $\mathbf{E}[\mathbf{n}_i \mathbf{n}_i^H] = N_0 \mathbf{I}_{N \times N}$. It can be shown that \mathbf{z}_i is a sufficient statistic for detecting the transmitted data. Using \mathbf{z}_i a MIMO receiver would perform detection of the transmitted data. Detection of the spatially multiplexed data which is not a focus of this study can be done for example, using the VBLAST algorithm [6, 47].

As a common practice, the detection procedure assumes that the channel response is perfectly estimated, and that $\hat{\mathbf{H}}$ corresponds to the true channel response. Let us

rewrite the expression in (2.17) as

$$\mathbf{z}_i = (\mathbf{H} + \mathbf{H}_e) \mathbf{d}_i + \frac{1}{A} \mathbf{n}_i - \mathbf{H}_e \mathbf{d}_i = \hat{\mathbf{H}} \mathbf{d}_i + \left(\frac{1}{A} \mathbf{n}_i - \mathbf{H}_e \mathbf{d}_i \right). \quad (2.18)$$

The effective noise in the detection procedure (as a spatial vector) is

$$\bar{\mathbf{n}}_i = \left(\frac{1}{A} \mathbf{n}_i - \mathbf{H}_e \mathbf{d}_i \right). \quad (2.19)$$

For the given $\hat{\mathbf{H}}$, the covariance matrix of the effective noise vector is

$$\mathbf{\Upsilon} = \mathbf{\Upsilon}(A) = \mathbb{E}_{\bar{\mathbf{n}}_i | \hat{\mathbf{H}}} [\bar{\mathbf{n}}_i \bar{\mathbf{n}}_i^H] = \frac{N_0}{A^2} \mathbf{I} + \mathbb{E}_{\mathbf{H}_e | \hat{\mathbf{H}}} [\mathbf{H}_e \mathbf{H}_e^H] \quad (2.20)$$

and it is a function of the amplitude A . As said earlier \mathbf{H}_e is a matrix of *iid* Gaussian random variables with distribution $\mathcal{N}_{\mathcal{C}}(0, N_0/(L(\alpha A)^2))$.

It can be shown that for a Rayleigh channel, where the entries of \mathbf{H} are *iid* Gaussian random variables with distribution $\mathcal{N}_{\mathcal{C}}(0, 1)$, the above covariance matrix is

$$\mathbf{\Upsilon} = \frac{N_0}{A^2} \mathbf{I} + M \frac{1}{1 + L(\alpha A)^2/N_0} \mathbf{I} + \left(\frac{1}{1 + L(\alpha A)^2/N_0} \right)^2 \hat{\mathbf{H}} \hat{\mathbf{H}}^H. \quad (2.21)$$

2.3 Estimates Available to Receiver:

Open Loop Capacity

Assuming that the channel response estimate is available to the receiver only, we determine the lower bound for the open loop ergodic capacity as follows.

$$C \geq R = \frac{K - LM}{K} \mathbb{E}_{\hat{\mathbf{H}}} \left[\log_2 \det \left(\mathbf{I}_{M \times M} + \hat{\mathbf{H}} \hat{\mathbf{H}}^H \mathbf{\Upsilon}^{-1} \right) \right]. \quad (2.22)$$

The term $(K - LM)/K$ is introduced because L temporal signature per each transmit antenna are allocated to the pilot. Also, the random process $\hat{\mathbf{H}}$ has to be stationary and ergodic (this is a common requirement for fading channel and ergodic capacity [43,51]).

We assume that the channel coding will span across great number of channel blocks (i.e., we use the well known infinite channel coding time horizon, required to achieve error-free data transmission with rates approaching capacity [52]).

In the above expression, equality holds if the effective noise (given in (2.19)) is AWGN with respect to the transmitted signal. If the effective noise is not AWGN,

then the above rates represent the worst-case scenario, i.e., the lower bound [38, 53]. In achieving the above rates, the receiver assumes that the effective noise is interference (which is independent of the transmitted data) with a Gaussian distribution and spatial covariance matrix $\mathbf{\Upsilon}$. In addition, in the above expression R represents an achievable rate for reliable transmission (error-free) for the specific estimation procedure assumed. Knowing the channel response perfectly or using a better channel estimation scheme (e.g., decision driven schemes) may result in higher achievable rates.

Note that the capacity lower bounds for MIMO channel estimation independently derived in [38] assume the time multiplexing of data and pilot (i.e., training) symbols. The authors also present analytical results on the optimal properties required of the training sequences, their duration and power. The signal model presented here is more general than that and the distinguishing feature of this study is the mismatched closed loop transmission analysis presented in the next section.

In the following we compare the above result in equation (2.22) to an information theoretic result presented in [43] (page 2641, expression (3.3.55)). The result is presented for the conventional SISO case, introducing a capacity lower bound for mismatched decoding as

$$C \geq R^* = \mathbb{E}_{\hat{h}} \left[\log_2 \left(1 + \frac{\hat{h}^2 P}{\mathbb{E}_{h|\hat{h}}(|h - \hat{h}|^2)P + N_0} \right) \right] \quad (2.23)$$

where h and \hat{h} are the SISO channel response and its estimate, respectively. The above result is quite general, not specifying the channel response estimation procedure. The bound in (2.22) is an extension of the information theoretic bound in (2.23), capturing the more practical pilot assisted channel response estimation scheme and generalizing it to the MIMO case. Consequently,

Proposition 1 *For the SISO case ($M = 1, N = 1$), the rate R in (2.22) and R^* in (2.23), are related as*

$$R = \frac{K - L}{K} R^*, \text{ for } P = \frac{K}{(K - L) + \alpha^2 L} P_{av} \quad (2.24)$$

where \hat{h} is obtained using the pilot assisted estimation.

2.4 Estimates Available to Transmitter and Receiver: Closed Loop Capacity

In MIMO systems, when the channel state \mathbf{H} is perfectly known at the transmitter, to maximize the capacity (under constrained transmit power), the transmitter performs optimization known as *the water pouring on eigen modes*. For SISO systems the water pouring algorithm is given in [54]. In practical communication systems, the channel state \mathbf{H} has to be estimated at the receiver, and then fed to the transmitter. In the case of a time varying channel, this practical procedure results in noisy and delayed (temporally mismatched) estimates being available to the transmitter to perform the optimization.

As said earlier, the MIMO channel is time varying. Let \mathbf{H}_{i-1} and \mathbf{H}_i correspond to consecutive block faded channel responses. In the following, the subscripts i and $i - 1$ on different variables will indicate values corresponding to the block channel periods i and $i - 1$, respectively. The temporal characteristic of the channel is described using the correlation

$$\text{E} \left[h_{(i-1)nm} h_{inm}^* \right] / \Gamma = \kappa, \quad (2.25)$$

where $\Gamma = \text{E}[h_{inm} h_{inm}^*]$, and h_{inm} is a stationary random process (for $m = 1, \dots, M$ and $n = 1, \dots, N$, denoting transmit and receive antenna indices, respectively). We assume that the value of the correlation κ is not known at the receiver and the transmitter. Note that the above channel is modeled as a first order discrete Markov process².

Adopting a practical scenario, we assume that the receiver feeds back the estimate $\hat{\mathbf{H}}_{i-1}$. Because the ideal channel state \mathbf{H}_i is not available at the transmitter, we assume that $\hat{\mathbf{H}}_{i-1}$ is used instead to perform the water pouring transmitter optimization for the i th block. In other words the transmitter is ignoring the fact that $\mathbf{H}_i \neq \hat{\mathbf{H}}_{i-1}$.

The water pouring optimization is performed as follows. First, the estimate is decomposed using singular value decomposition (SVD) as $\hat{\mathbf{H}}_{i-1} = \hat{\mathbf{U}}_{i-1} \hat{\mathbf{\Sigma}}_{i-1} \hat{\mathbf{V}}_{i-1}^H$ [55]. Then, if the data vector $\mathbf{d}(k)$ is to be transmitted (in equation (2.4)), the following

²Note that in the case of the Jakes model, $\kappa = J_0(2\pi f_d \tau)$, where f_d is the maximum Doppler frequency and τ is the time difference between $h_{(i-1)nm}$ and h_{inm} .

linear transformation is performed at the transmitter

$$\bar{\mathbf{d}}(k) = \widehat{\mathbf{V}}_{i-1} \mathbf{S}_i \mathbf{d}(k), \quad (2.26)$$

where the matrix \mathbf{S}_i is a diagonal matrix whose elements s_{ijj} ($j = 1, \dots, M$) are determined by the water pouring algorithm per singular value of $\widehat{\mathbf{H}}_{i-1}$, i.e., the diagonal element of $\widehat{\Sigma}_{i-1}$ (denoted as $\hat{\sigma}_{(i-1)jj}$, $j = 1, \dots, M$). The diagonal element of \mathbf{S}_i is defined as

$$s_{ijj}^2 = \begin{cases} \frac{1}{\gamma_0} - \frac{N_0}{|\hat{\sigma}_{(i-1)jj}|^2 A^2} & \text{for } |\hat{\sigma}_{(i-1)jj}|^2 A^2 / N_0 \geq \gamma_0 \\ 0 & \text{otherwise} \end{cases} \quad (2.27)$$

γ_0 is a *cut-off* value, and it depends on the channel fading statistics. It is selected such that the average transmit power stays the same P_{av} [54]. Consequently, at the time instant k , the received spatial vector is

$$\mathbf{y}(k) = \mathbf{H}_i \widehat{\mathbf{V}}_{i-1} \mathbf{S}_i \mathbf{d}(k) + \mathbf{H}_i \mathbf{p}(k) + \mathbf{n}(k) = \mathbf{G} \mathbf{d}(k) + \mathbf{H}_i \mathbf{p}(k) + \mathbf{n}(k) \quad (2.28)$$

and

$$\mathbf{G} = \mathbf{H}_i \widehat{\mathbf{V}}_{i-1} \mathbf{S}_i. \quad (2.29)$$

The water pouring optimization is applied on the data bearing portion of the signal $\mathbf{d}(k)$, while the pilot $\mathbf{p}(k)$ is not changed. The receiver knows that the transformation in (2.26) is performed at the transmitter. The receiver performs estimation of the channel response matrix as given in section 2.2, resulting in $\widehat{\mathbf{G}} = \widehat{\mathbf{H}}_i \widehat{\mathbf{V}}_{i-1} \mathbf{S}_i$ and the error matrix $\mathbf{G}_e = \mathbf{H}_{e_i} \widehat{\mathbf{V}}_{i-1} \mathbf{S}_i$. In this case, the effective noise in (2.19) and its covariance matrix in (2.20) are modified accordingly resulting in

$$\mathbf{\Upsilon}^{WP} = \mathbf{\Upsilon}^{WP}(A) = \frac{N_0}{A^2} \mathbf{I} + E_{\mathbf{G}_e | \widehat{\mathbf{G}}} [\mathbf{G}_e \mathbf{G}_e^H]. \quad (2.30)$$

In the above and following expressions the superscript "WP" denotes *water pouring*. Note that the above application of the water pouring algorithm per eigen mode is suboptimal, i.e., it is mismatched (because $\widehat{\mathbf{H}}_{i-1}$ is used instead of \mathbf{H}_i). Consequently, the closed loop system capacity is bounded as,

$$C^{WP} \geq R^{WP} = \frac{K - LM}{K} E_{\widehat{\mathbf{G}}} \left[\log_2 \det \left(\mathbf{I}_{M \times M} + \widehat{\mathbf{G}} \widehat{\mathbf{G}}^H (\mathbf{\Upsilon}^{WP})^{-1} \right) \right]. \quad (2.31)$$

Similar to the comments related to the result in (2.22), the random process $\widehat{\mathbf{G}}$ has to be stationary and ergodic. Also, the channel coding will span across infinite number of channel blocks to achieve error-free data transmission approaching the above rates. Again, the equality holds if the effective noise is AWGN with respect to the transmitted signal and if not, then the above rates represent the worst-case scenario, i.e., the lower bound [53]. In achieving the above rates, the receiver assumes that the effective noise is interference which is independent of the transmitted data with Gaussian distribution and spatial covariance matrix $\mathbf{\Upsilon}^{WP}$. Knowing the channel response perfectly or using a better channel estimation, or prediction scheme may result in higher achievable rates. There has also been some recent work in [56] on closed loop MIMO OFDM transmission over a parametric frequency selective channel model.

2.5 Examples and Numerical Results

2.5.1 SISO Systems

To illustrate the above analysis we start with SISO systems. In the SISO case, all previously defined spatial vectors and related matrices are now single dimensional (e.g., \mathbf{d}_i , \mathbf{H} , $\widehat{\mathbf{H}}$ and $\mathbf{\Upsilon}$ are now scalars d_i , h , \hat{h} and v , respectively). In Figure 2.1, we present the rate R in (2.22) as a function of the power allocated to the pilot (equation (2.10)). In this example, a pilot period K is 10 and coincides with the coherence time. A frequency-flat Rayleigh fading channel is assumed. The results are shown for the pilot arrangements corresponding to both case 1 and case 2. For ideal knowledge of the channel response we apply the ergodic capacity formula [43]. Regarding the achievable rates, from the above results we observe that case 1 is less sensitive to the pilot power allocation than case 2 (i.e., in case 2, R is dropping faster if the allocated power is different than the one that results in the maximum value). Further, case 1 is achieving higher maximum achievable rates than case 2.

For the given SNR , we define the capacity efficiency ratio η as the ratio between the maximum rate R (maximized with respect to the pilot power) and the ergodic capacity

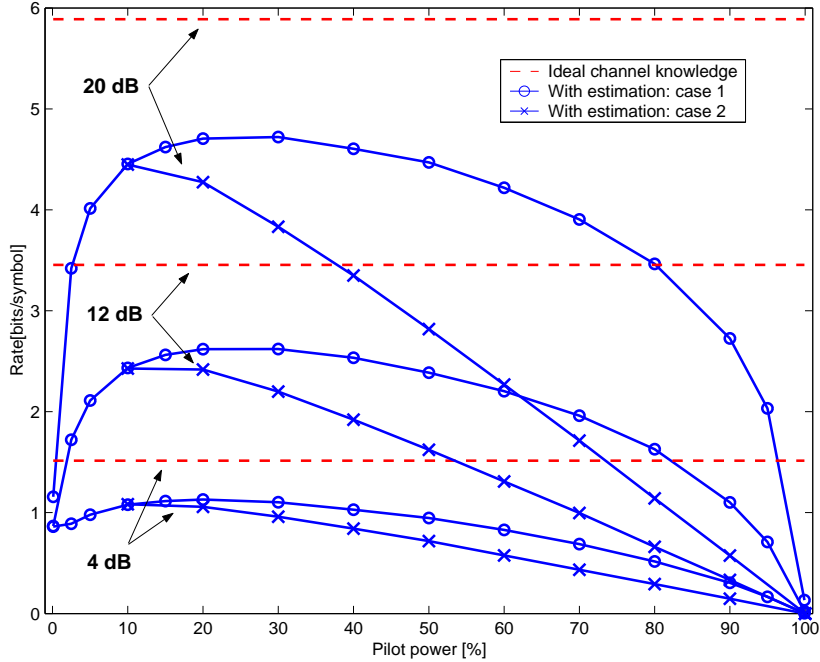


Figure 2.1: Achievable open loop rates vs. power allocated to the pilot, SISO system, $SNR = 4, 12, 20\text{dB}$, coherence time $K = 10$, Rayleigh channel.

$C_{m \times n}$ in the case of the ideal knowledge of the channel response, i.e.,

$$\eta_{m \times n} = \frac{\max_{\mu} R}{C_{m \times n}}. \quad (2.32)$$

The index m and n correspond to number of transmit and receive antennas, respectively. In Figure 2.2, we show that the capacity efficiency ratio $\eta_{1 \times 1}$ increases with the channel coherence time. From the above results we conclude that case 1 is a more efficient scheme than case 2.

2.5.2 MIMO Systems

In Figure 2.3, we present the rate R in (2.22) as a function of the power allocated to the pilot (equation (2.10)), for different number of transmit and receive antennas. In this and the following numerical examples we consider only the pilot arrangement case 1 (viewing case 2 as impractical for MIMO systems). We observe the rates for the Rayleigh channel, $SNR = 12\text{dB}$ and the channel coherence time length $K = 40$. Solid lines correspond to a system with the channel response estimation, and dashed

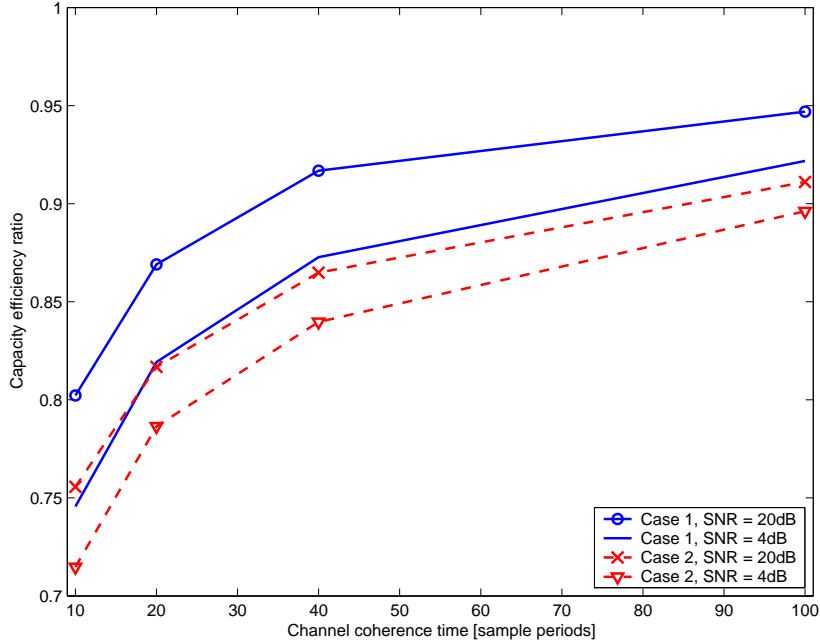


Figure 2.2: Capacity efficiency ratio vs. channel coherence time ($K = 10, 20, 40, 100$), SISO system, $SNR = 4, 20\text{dB}$, Rayleigh channel.

lines to a system with the ideal knowledge of the channel response. Further, in Figure 2.4 we show the capacity efficiency ratio η for different number of transmit and receive antennas vs. different channel coherence time lengths. We observe that as the number of transmit antennas increase, the sensitivity to the channel response estimation error is more pronounced (while keeping the same number of receive antennas). For example, for the same channel coherence time length, the capacity efficiency ratio of the 4×4 system is lower than that in the case of the 3×4 system.

In Figure 2.5 we present open loop (solid lines) and closed loop (dashed lines) ergodic capacities. Idealized conditions are assumed, i.e., the ideal knowledge of the channel response is available to the transmitter and receiver and perfect temporal match $\mathbf{H}_{i-1} = \mathbf{H}_i$ (for the water pouring optimization) is assumed. Comparing the closed loop and open loop capacity, we observe that the gains are more pronounced for lower SNR (e.g, for 4×4 system at 0dB, the gain of the closed loop system is approximately 2dB, while at 12dB, it drops below 0.5dB). Further, we note that in the case of 2×4 and 1×4 systems, the gain practically disappears. This is explained as an effect of

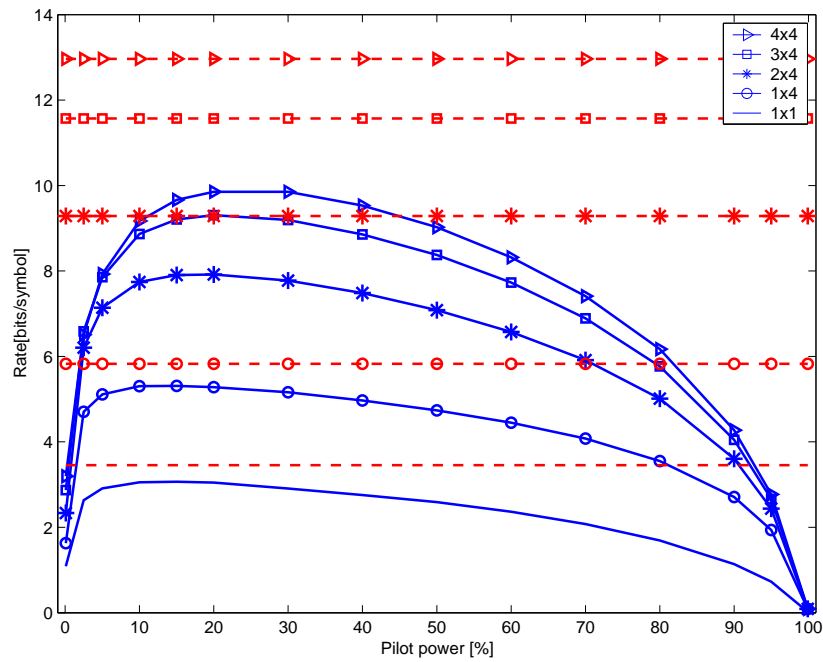


Figure 2.3: Achievable open loop rates vs. power allocated to the pilot, MIMO system, $SNR = 12\text{dB}$, coherence time $K = 40$, Rayleigh channel, solid line corresponds to a system with the channel response estimation, and dashed line to the case of the ideal channel response knowledge.

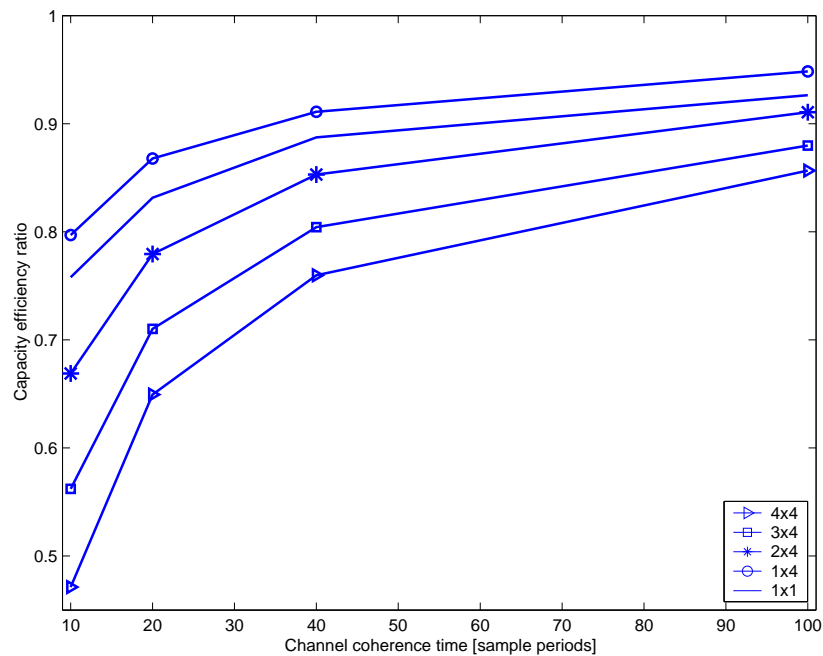


Figure 2.4: Capacity efficiency ratio vs. channel coherence time ($K = 10, 20, 40, 100$), MIMO system, $SNR = 12\text{dB}$, Rayleigh channel.

multiple receive antennas (greater than the number of transmit antennas) providing already sufficient degree of diversity, eliminating any need for transmitter optimization. Instead of the ergodic capacities, when observing the cumulative distribution function (cdf) of the capacity, the difference is more pronounced (Figure 2.6, for $SNR = 4\text{dB}$) (see more on the "capacity versus outage" approach in [43]).

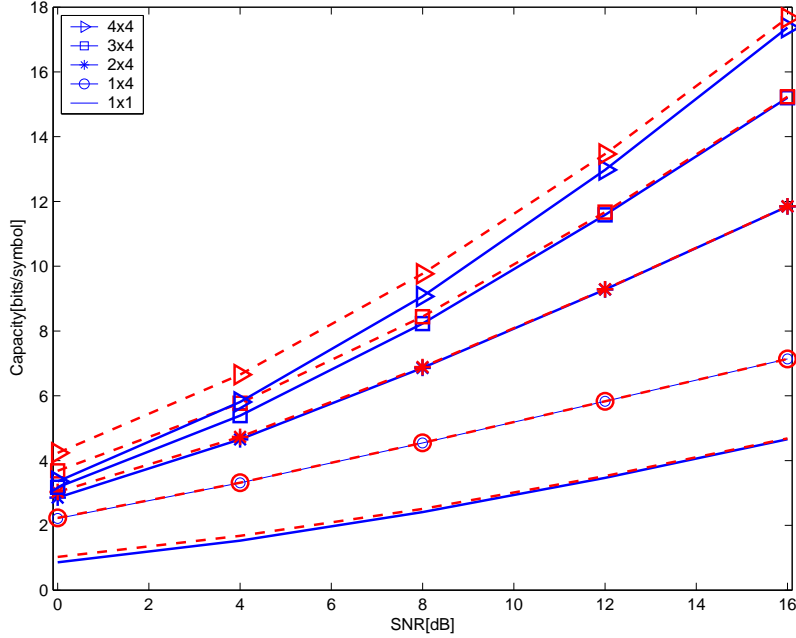


Figure 2.5: Ergodic capacity vs. SNR, MIMO system, ideal knowledge of the channel response, Rayleigh channel, solid line corresponds to open loop capacity, and dashed line to closed loop capacity (perfect temporal match $\mathbf{H}_{i-1} = \mathbf{H}_i$ is assumed).

From the results in Figure 2.7, we observe how the temporal mismatch between successive channel responses ($\mathbf{H}_{i-1} \neq \mathbf{H}_i$) affects the achievable rates R^{WP} in (2.31). As said earlier, the temporal mismatch is characterized by the correlation κ . We observe the cases when the ideal channel response (dashed lines) and channel response estimates (solid lines) are available at the transmitter and the receiver. Solid lines correspond to the channel response estimation where the pilot power is selected to maximize the achievable rate R^{WP} . We observe the rates for the Rayleigh channel, $SNR = 4\text{dB}$ and the coherence time length $K = 40$. Note that for $\kappa = 0$ (i.e., when the successive channel responses are uncorrelated), the achievable rate is lower than in the case of $\kappa = 1$ (i.e., when the successive channel responses are fully correlated). The drop in

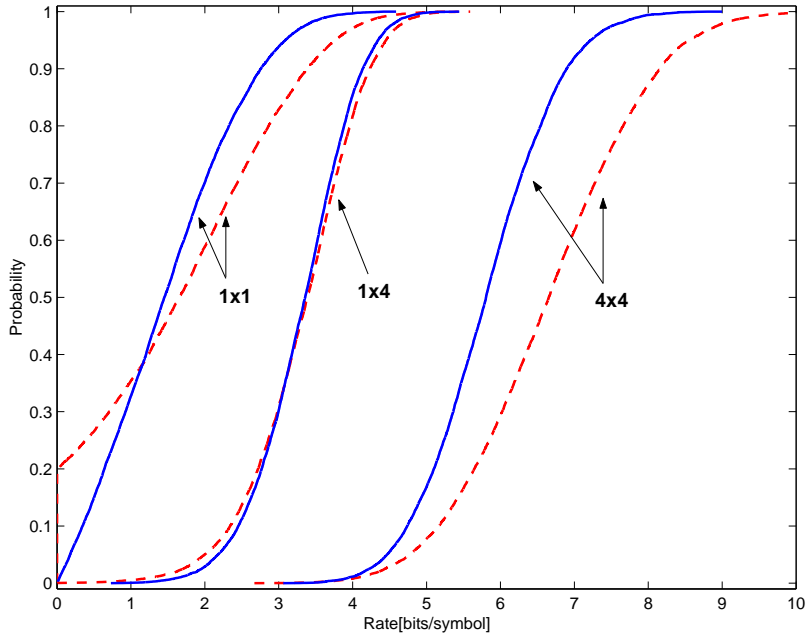


Figure 2.6: CDF of capacity, MIMO system, $SNR = 4\text{dB}$, ideal knowledge of the channel response, Rayleigh channel, solid line corresponds to open loop capacity, and dashed line to closed loop capacity (perfect temporal match $\mathbf{H}_{i-1} = \mathbf{H}_i$ is assumed).

the achievable rates is not substantial, even though the water pouring algorithm is fully mismatched for $\kappa = 0$. We explain this behavior in the following. In the case of a Rayleigh channel, the matrix $\hat{\mathbf{V}}_{i-1}\mathbf{S}_i$ usually has M degrees of freedom, and a small condition number of the corresponding covariance matrix. Consequently, even in the mismatched case, multiplying \mathbf{H}_i with $\hat{\mathbf{V}}_{i-1}\mathbf{S}_i$ preserves the degrees of freedom of the matrix \mathbf{H}_i resulting in a high capacity of the composite channel \mathbf{G} in (2.29). We expect the detrimental effects of the mismatch to be amplified in the case of Rician channels, especially those with large K-factor. This is because Rician channels result in the matrix $\hat{\mathbf{V}}_{i-1}\mathbf{S}_i$ having a few dominant degrees of freedom thereby making accurate feedback beneficial.

In Figure 2.8 we compare the open loop scheme to the closed loop scheme under temporal mismatch. It is observed that when the channel coherence is low (i.e., low correlation κ), it is better to not use a closed loop scheme. In the observed case (4×4 , $SNR = 4\text{dB}$ and coherence time $K = 40$), for the correlation coefficient $\kappa < 0.7$ the achievable rates for the closed loop scheme are lower than in the open loop case.

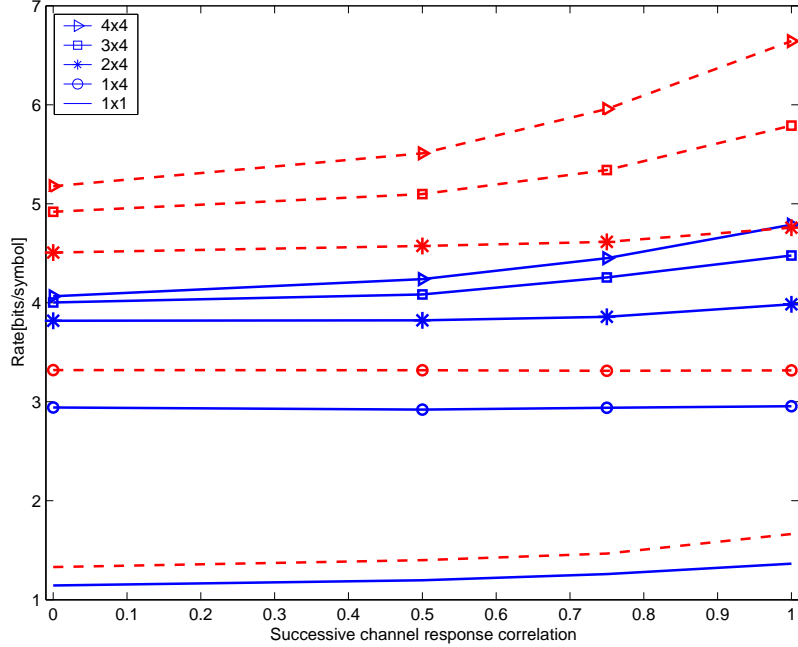


Figure 2.7: Achievable closed loop rates vs. correlation between successive channel responses, MIMO system, $SNR = 4\text{dB}$, coherence time $K = 40$, Rayleigh channel, solid line corresponds to a system with the channel response estimation, and dashed line to the case of the ideal channel response available at the transmitter and the receiver (but with the temporal mismatched $\mathbf{H}_{i-1} \neq \mathbf{H}_i$).

2.6 Conclusion

In this chapter we have studied how the estimation error of the frequency-flat time-varying channel response affects the performance of a MIMO communication system. Using a block-fading channel model, we have connected results of information theory with practical pilot estimation for such systems. The presented analysis may be viewed as a study of mismatched receiver and transmitter algorithms in MIMO systems. We have considered two pilot based schemes for the estimation. The first scheme uses a single pilot symbol per block with different power than the data symbol power. The second scheme uses more than one pilot symbol per block, whose power is the same as the data symbol power. We have presented how the achievable data rates depend on the percentage of the total power allocated to the pilot, background noise level and

the channel coherence time length. Our results have shown that the first pilot-based approach is less sensitive to the fraction of power allocated to the pilot. Furthermore, we have observed that as the number of transmit antennas increase, the sensitivity to the channel response estimation error is more pronounced (while keeping the same number of receive antennas). The effects of the estimation error are evaluated in the case of the estimates being available at the receiver only (open loop), and in the case when the estimates are fed back to the transmitter (closed loop) allowing water pouring transmitter optimization. In the case of water pouring transmitter optimization and corresponding rates, we have not observed significant gains versus the open loop rates for the channel models considered here. Further, we observe that in certain cases, it is better to use the open loop scheme as opposed to the closed loop scheme. The analysis presented here can be used to optimally allocate pilot power for various system and channel operating conditions, and to also determine the effectiveness of closed loop feedback.

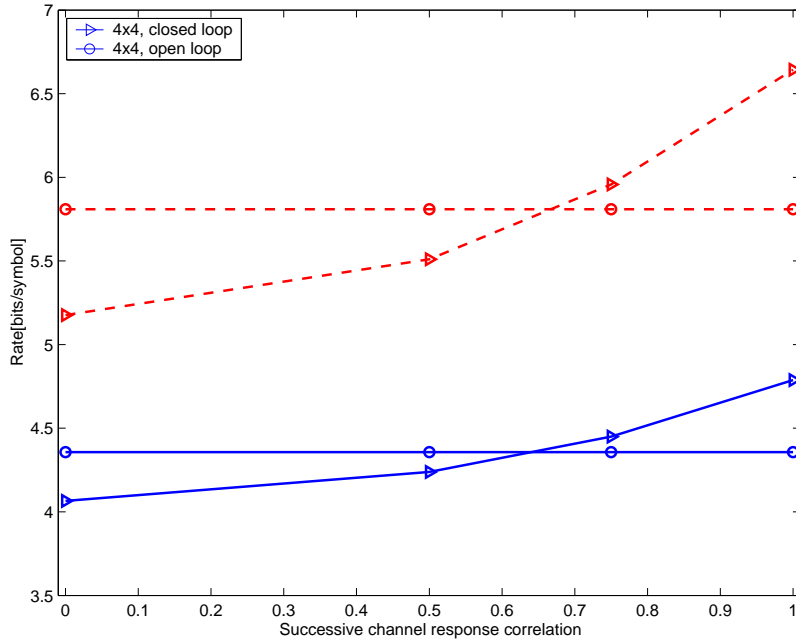


Figure 2.8: Achievable closed loop and open loop rates vs. correlation between successive channel responses, MIMO system 4×4 , $SNR = 4\text{dB}$, coherence time $K = 40$, Rayleigh channel, solid line corresponds to a system with the channel response estimation, and dashed line to the case of the ideal channel response available at the transmitter and the receiver (but with the temporal mismatched $\mathbf{H}_{i-1} \neq \mathbf{H}_i$).

Chapter 3

Downlink Multiple Antenna Transmitter Optimization on Spatially and Temporally Correlated Channels with Delayed Channel State Information

Recently there have been a lot of efforts in using multiple antennas to achieve performance gains in systems with multiple users (see [25–27, 32, 33] and references therein). In this chapter we study multiple antenna transmitter optimization (i.e., spatial pre-filtering) schemes that are based on linear transformations and transmit power optimization (keeping the average transmit power conserved). We consider the downlink of a wireless system with multiple transmit antennas at the base station and a number of mobile terminals (i.e., users) each with a single receive antenna. From an information theoretic model, the downlink corresponds to the case of a *broadcast channel* [57]. We consider the maximum achievable sum data rates in the case of (1) zero-forcing spatial pre-filter, (2) modified zero-forcing spatial pre-filter and (3) triangularization spatial pre-filtering coupled with dirty paper coding transmission scheme [40]. To the best of our knowledge, most of the previously reported studies assume perfect knowledge of the channel state (i.e., response) at the transmitter. Transmitter beamforming solutions that use partial knowledge of the channel (i.e., its mean and variance) have also been studied [58]. In this chapter we study the performance of the transmitter optimization schemes with respect to delayed CSI. A multiple input single output (MISO) channel model is introduced modeling temporal and spatial correlations. We show how the performance of the schemes depends on spatial correlations and the CSI delay. To exploit spatial and temporal correlations a linear MMSE predictor of the channel state is introduced. We show that the application of the MMSE predictor can further improve performance of the schemes for delayed CSI.

3.1 System Model and Transmitter Optimization Schemes

In the following we introduce the system model. We use a MIMO model [1] that corresponds to a system presented in Figure 3.1. It consists of M transmit antennas and N mobile terminals. In other words each mobile terminal presents a MISO channel as seen from the base station.

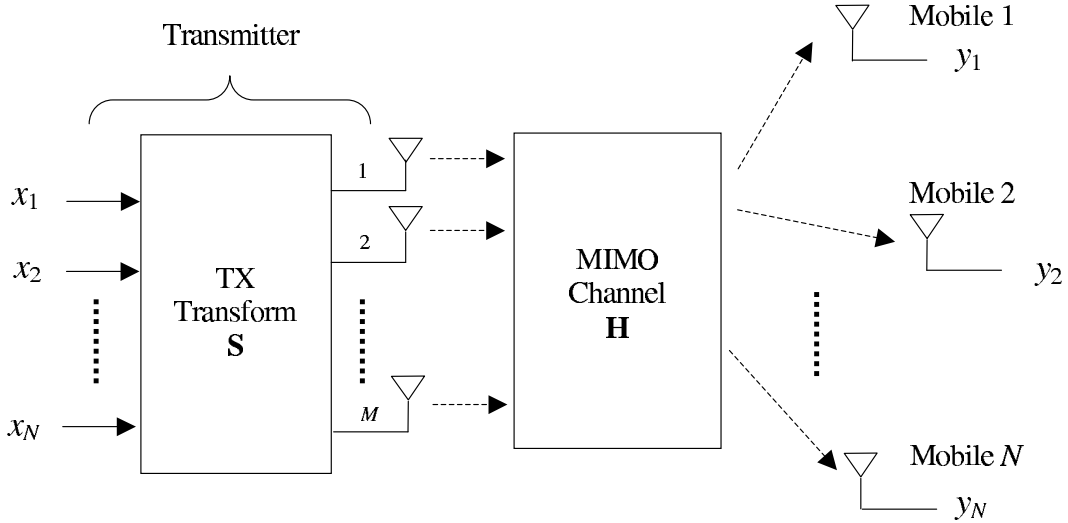


Figure 3.1: System model consisting of M transmit antennas and N mobile terminals.

In Figure 3.1, x_n is the information bearing signal intended for mobile terminal n and y_n is the received signal at the corresponding terminal (for $n = 1, \dots, N$). The received vector $\mathbf{y} = [y_1, \dots, y_N]^T$ is

$$\begin{aligned} \mathbf{y} &= \mathbf{H}\mathbf{S}\mathbf{x} + \mathbf{n}, \\ \mathbf{y} &\in \mathcal{C}^N, \mathbf{x} \in \mathcal{C}^N, \mathbf{n} \in \mathcal{C}^N, \mathbf{S} \in \mathcal{C}^{M \times N}, \mathbf{H} \in \mathcal{C}^{N \times M} \end{aligned} \quad (3.1)$$

where $\mathbf{x} = [x_1, \dots, x_N]^T$ is the transmitted vector ($E[\mathbf{x}\mathbf{x}^H] = P_{av} \mathbf{I}_{N \times N}$), \mathbf{n} is AWGN ($E[\mathbf{n}\mathbf{n}^H] = N_0 \mathbf{I}_{N \times N}$), \mathbf{H} is the MIMO channel response matrix, and \mathbf{S} is a transformation (spatial pre-filtering) performed at the transmitter. Note that the vectors \mathbf{x} and \mathbf{y} have the same dimensionality. Further, h_{nm} is the n th row and m th column element of the matrix \mathbf{H} corresponding to a channel between mobile terminal n and transmit antenna m .

Application of the spatial pre-filtering results in the composite MIMO channel \mathbf{G}

given as

$$\mathbf{G} = \mathbf{H}\mathbf{S}, \quad \mathbf{G} \in \mathcal{C}^{N \times N} \quad (3.2)$$

where g_{nm} is the n th row and m th column element of the composite MIMO channel response matrix \mathbf{G} . The signal received at the n th mobile terminal is

$$y_n = \underbrace{g_{nn}x_n}_{\text{Desired signal for user } n} + \underbrace{\sum_{i=1, i \neq n}^N g_{ni}x_i}_{\text{Interference}} + n_n. \quad (3.3)$$

In the above representation, the interference is the signal that is intended for other mobile terminals than terminal n . As said earlier, the matrix \mathbf{S} is a spatial pre-filter at the transmitter. It is determined based on optimization criteria that we address later in the text and has to satisfy the following constraint

$$\text{trace}(\mathbf{S}\mathbf{S}^H) \leq N \quad (3.4)$$

which keeps the average transmit power conserved. We represent the matrix \mathbf{S} as

$$\mathbf{S} = \mathbf{A}\mathbf{P}, \quad \mathbf{A} \in \mathcal{C}^{M \times N}, \mathbf{P} \in \mathcal{C}^{N \times N} \quad (3.5)$$

where \mathbf{A} is a linear transformation and \mathbf{P} is a diagonal matrix. \mathbf{P} is determined such that the transmit power remains conserved. Considering different forms of the matrix \mathbf{A} we study the following solutions.

1. Zero-forcing (ZF) spatial pre-filtering scheme where \mathbf{A} is represented by

$$\mathbf{A} = \mathbf{H}^H(\mathbf{H}\mathbf{H}^H)^{-1}. \quad (3.6)$$

As can be seen, the above linear transformation is zeroing the interference between the signals dedicated to different mobile terminals, i.e., $\mathbf{H}\mathbf{A} = \mathbf{I}_{N \times N}$. The x_n 's are assumed to be circularly symmetric complex random variables having Gaussian distribution $\mathcal{N}_{\mathcal{C}}(0, P_{av})$. Consequently, the maximum achievable data rate (capacity) for mobile terminal n is

$$R_n^{\text{ZF}} = \log_2 \left(1 + \frac{P_{av}|p_{nn}|^2}{N_0} \right) \quad (3.7)$$

where p_{nn} is the n th diagonal element of the matrix \mathbf{P} defined in (3.5). In (3.6) it is assumed that $\mathbf{H}\mathbf{H}^H$ is invertible, i.e, the rows of \mathbf{H} are linearly independent.

2. Modified zero-forcing (MZF) spatial pre-filtering scheme that assumes

$$\mathbf{A} = \mathbf{H}^H \left(\mathbf{H}\mathbf{H}^H + \frac{N_0}{P_{av}} \mathbf{I} \right)^{-1}. \quad (3.8)$$

In the case of the above transformation, in addition to the knowledge of the channel \mathbf{H} the transmitter has to know the noise variance N_0 . The x_n 's are assumed to be circularly symmetric complex random variables having Gaussian distribution $\mathcal{N}_C(0, P_{av})$. The maximum achievable data rate (capacity) for mobile terminal n now becomes

$$R_n^{\text{MZF}} = \log_2 \left(1 + \frac{P_{av} |g_{nn}|^2}{P_{av} \sum_{i=1, i \neq n}^N |g_{ni}|^2 + N_0} \right). \quad (3.9)$$

While the transformation in (3.8) appears to be similar in form to a MMSE linear receiver, the important difference is that the transformation is performed at the transmitter. Using the virtual uplink approach for transmitter beamforming (introduced in [32,33]) we present the following proposition.

Proposition 2 *If the n th diagonal element of \mathbf{P} is selected as*

$$p_{nn} = \frac{1}{\sqrt{\mathbf{a}_n^H \mathbf{a}_n}} \quad (n = 1, \dots, N) \quad (3.10)$$

where \mathbf{a}_n is the n th column vector of the matrix \mathbf{A} , the constraint in (3.4) is satisfied with equality. Consequently, the achievable downlink rate R_n^{MZF} for mobile n is identical to its corresponding virtual uplink rate when an optimal uplink linear MMSE receiver is applied.

See Appendix A for a definition of the corresponding virtual uplink and a proof of the above proposition.

3. Triangularization spatial pre-filtering with dirty paper coding (DPC) where the matrix \mathbf{A} assumes the form

$$\mathbf{A} = \mathbf{H}^H \mathbf{R}^{-1} \quad (3.11)$$

where $\mathbf{H} = (\mathbf{Q}\mathbf{R})^H$ and \mathbf{Q} is unitary and \mathbf{R} is upper triangular (see [55] for details on QR factorization). In general, \mathbf{R}^{-1} is a pseudo inverse of \mathbf{R} . The composite

MIMO channel \mathbf{G} in (3.2) becomes $\mathbf{G} = \mathbf{L} = \mathbf{H}\mathbf{S}$, a lower triangular matrix. It permits application of dirty paper coding designed for single input single output (SISO) systems. We refer the reader to [25–27, 59–62] for further details on the DPC schemes.

By applying the transformation in (3.11), the signal intended for terminal 1 is received without interference. The signal at terminal 2 suffers from the interference arising from the signal dedicated to terminal 1. In general, the signal at terminal n suffers from the interference arising from the signals dedicated to terminals 1 to $n - 1$. In other words,

$$\begin{aligned}
 y_1 &= g_{11}x_1 + n_1, \\
 y_2 &= g_{22}x_2 + g_{21}x_1 + n_2, \\
 &\vdots \\
 y_n &= g_{nn}x_n + \sum_{i=1}^{n-1} g_{ni}x_i + n_n, \\
 &\vdots \\
 y_N &= g_{NN}x_N + \sum_{i=1}^{N-1} g_{Ni}x_i + n_N.
 \end{aligned} \tag{3.12}$$

Since the interference is known at the transmitter, DPC can be applied to mitigate the interference (the details are given in Appendix B). Based on the results in [59], the achievable rate for mobile terminal n is

$$R_n^{\text{DPC}} = \log_2 \left(1 + \frac{P_{av}|g_{nn}|^2}{N_0} \right) = \log_2 \left(1 + \frac{P_{av}|r_{nn}p_{nn}|^2}{N_0} \right) \tag{3.13}$$

where r_{nn} is the n th diagonal element of the matrix \mathbf{R} defined in (3.11). Note that DPC is applied just in the case of the linear transformation in (3.11), with corresponding rate given by (3.13).

Note that $\text{trace}(\mathbf{A}\mathbf{A}^H) = N$, thereby satisfying the constraint in (3.4). Consequently, we can select $\mathbf{P} = \mathbf{I}_{N \times N}$ and present the following proposition.

Proposition 3 *For high SNR ($P_{av} \gg N_0$) and $\mathbf{P} = \mathbf{I}_{N \times N}$, the achievable sum rate of the triangularization with DPC scheme is equal to the rate of the equivalent*

(open loop) MIMO system. In other words, for $P_{av} \gg N_0$

$$\sum_{n=1}^N R_n^{\text{DPC}} = \log_2 \left(\det \left(\mathbf{I}_{N \times N} + \frac{P_{av}}{N_0} \mathbf{H} \mathbf{H}^H \right) \right). \quad (3.14)$$

Proof: Starting from the right side term in (3.14) and with $\mathbf{H} \mathbf{H}^H = \mathbf{R}^H \mathbf{R}$, for $P_{av} \gg N_0$

$$\begin{aligned} & \log_2 \left(\det \left(\mathbf{I}_{N \times N} + \frac{P_{av}}{N_0} \mathbf{R}^H \mathbf{R} \right) \right) \approx \\ & \approx \log_2 \left(\det \left(\frac{P_{av}}{N_0} \mathbf{R}^H \mathbf{R} \right) \right) = \\ & = \log_2 \left(\frac{P_{av}}{N_0} |r_{11}|^2 \cdots \frac{P_{av}}{N_0} |r_{NN}|^2 \right) = \\ & = \sum_{i=1}^N \log_2 \left(\frac{P_{av}}{N_0} |r_{ii}|^2 \right) \approx \\ & \approx \sum_{i=1}^N \log_2 \left(1 + \frac{P_{av}}{N_0} |r_{ii}|^2 \right) = \\ & = \sum_{n=1}^N R_n^{\text{DPC}} \end{aligned} \quad (3.15)$$

which concludes the proof. \square

The ZF and MZF schemes should be viewed as transmitter beamforming techniques using conventional channel coding to approach the achievable rates [32,33]. The triangularization with DPC scheme is necessarily coupled with a non-conventional coding, i.e., the DPC scheme.

Once the matrix \mathbf{A} is selected, the elements of the diagonal matrix \mathbf{P} are determined such that the transmit power remains conserved and the sum rate is maximized. The constraint on the transmit power is

$$\text{trace} \left(\mathbf{A} \mathbf{P} \mathbf{P}^H \mathbf{A}^H \right) \leq N. \quad (3.16)$$

The elements of the matrix \mathbf{P} are selected such that

$$\text{diag}(\mathbf{P}) = [p_{11}, \dots, p_{NN}]^T = \arg \max_{\text{trace}(\mathbf{A} \mathbf{P} \mathbf{P}^H \mathbf{A}^H) \leq N} \sum_{i=1}^N R_n. \quad (3.17)$$

Numerical Results

To evaluate the performance of the above schemes we consider the following baseline solutions.

1. *No pre-filtering* is a solution where each mobile terminal is served by one transmit antenna dedicated to that mobile. This is equivalent to $\mathbf{S} = \mathbf{I}$. A transmit antenna is assigned to a particular terminal corresponding to the best channel (maximum channel magnitude) among all available transmit antennas and that terminal.
2. *Equal resource TDMA and coherent beamforming* (denoted as TDMA-CBF) is a solution where signals for different terminals are sent in different (isolated) time slots. In this case, there is no interference, and each terminal is using $1/N$ of the overall resources. When serving a particular mobile, ideal coherent beamforming is applied using all M transmit antennas.
3. *Closed loop MIMO* (using the water pouring optimization on eigen modes) is a solution that is used as an upper bound on the achievable sum rates. In the following it is denoted as CL-MIMO. This solution would require that multiple terminals act as a joint multiple antenna receiver. This solution is not practical because the terminals are normally individual entities in the network and they do not cooperate when receiving signals on the downlink.

In Figure 3.2 we present average rates per user versus $SNR = 10 \log(P_{av}/N_0)$ for a system consisting of $M = 3$ transmit antennas and $N = 3$ terminals. The channel is Rayleigh, i.e., the elements of the matrix \mathbf{H} are complex independent identically distributed Gaussian random variables with distribution $\mathcal{N}_{\mathcal{C}}(0, 1)$. From the figure we observe the following. The triangularization with DPC scheme is approaching the closed loop MIMO rates for higher SNR. The MZF solution is performing very well for lower SNRs (approaching CL-MIMO and DPC rates), while for higher SNRs the rates for the ZF scheme are converging to the MZF rates. The TDMA-CBF rates are increasing with SNR, but still significantly lower than the rates of the proposed optimization schemes. The solution where no pre-filtering is applied clearly exhibits properties of

an interference limited system (i.e., after a certain SNR, the rates are not increasing). Corresponding cumulative distribution functions (cdf) of the sum rates normalized by the number of users are given in Figure 3.3, for $SNR = 10\text{dB}$ (see more on the "capacity versus outage" approach in [43]).

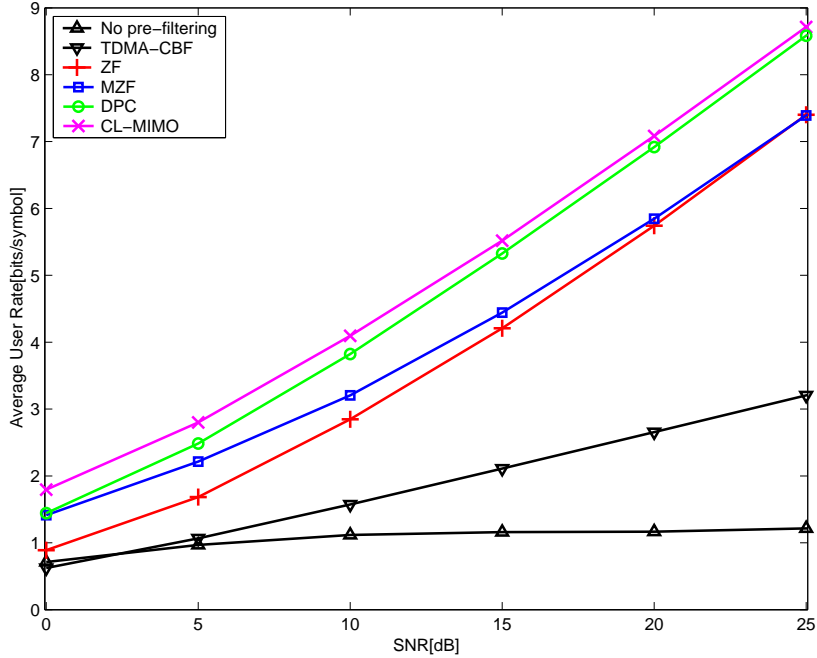


Figure 3.2: Average rate per user vs. SNR, $M = 3$, $N = 3$, Rayleigh channel.

In Figure 3.4 we present the behaviour of the average rate per user vs. number of transmit antennas. The average rates are observed for $SNR = 10\text{dB}$, $N = 3$, and a variable number of transmit antennas ($M = 3, 6, 12, 24$). The rates increase with the number of transmit antennas and the difference between the rates for different schemes becomes smaller.

As a motivation for the analysis presented in the following sections, we now present the effects of imperfect channel state knowledge. In practical communication systems, the channel state \mathbf{H} has to be estimated at the receivers, and then fed to the transmitter. Specifically, mobile terminal n feeds back the estimate of the n th row of the matrix \mathbf{H} , for $n = 1, \dots, N$. In the case of a time varying channel, this practical procedure results in noisy and delayed (temporally mismatched) estimates being available to the

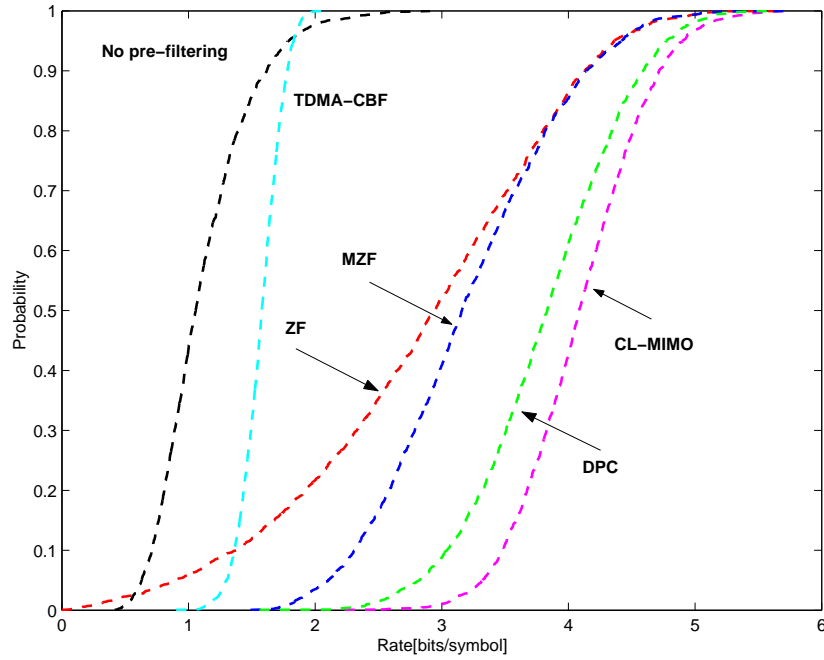


Figure 3.3: CDF of rates, $SNR = 10\text{dB}$, per user, $M = 3$, $N = 3$, Rayleigh channel.

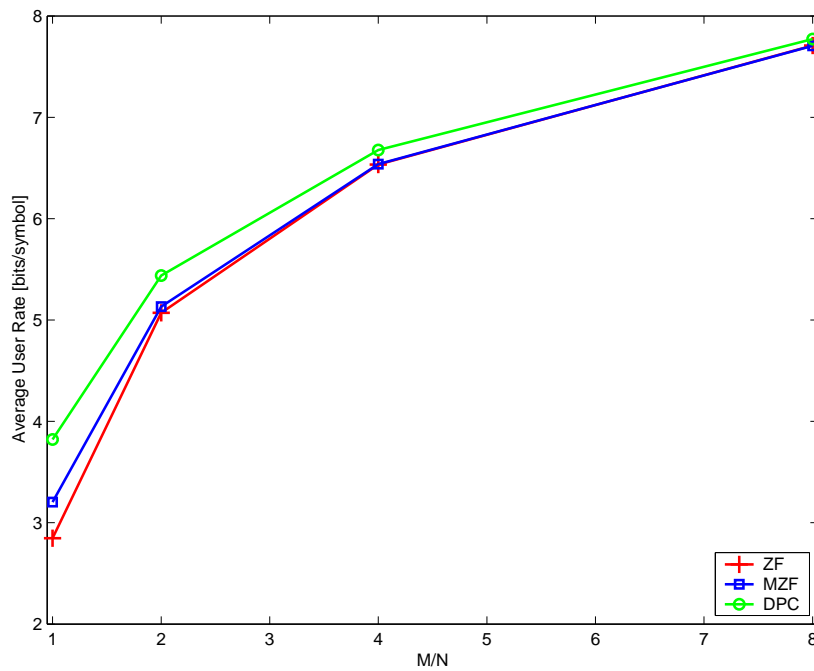


Figure 3.4: Average rate per user vs. M/N , $SNR = 10\text{dB}$, $N = 3$, variable number of transmit antenna $M = 3, 6, 12, 24$, Rayleigh channel.

transmitter to perform the optimization. As said earlier, the MIMO channel is time varying. Let \mathbf{H}_{i-1} and \mathbf{H}_i correspond to consecutive block faded channel responses. The temporal characteristic of the channel is described using the correlation

$$k = \text{E} \left[h_{(i-1)nm} h_{inm}^* \right] / \Gamma \quad (3.18)$$

where $\Gamma = \text{E}[h_{inm}h_{inm}^*]$, and h_{inm} is a stationary random process (for $m = 1, \dots, M$ and $n = 1, \dots, N$, denoting transmit and receive antenna indices, respectively). Low values of the correlation k correspond to higher mismatch between \mathbf{H}_{i-1} and \mathbf{H}_i . Note that the above channel is modeled as a first order discrete Markov process. In the case of the Jakes model, $k = J_0(2\pi f_d \tau)$, where f_d is the maximum Doppler frequency and τ is the time difference between $h_{(i-1)nm}$ and h_{inm} . In addition, the above simplified model assumes that there is no spatial correlation.

We assume that the mobile terminals feed back \mathbf{H}_{i-1} which is used at the base station to perform the transmitter optimization for the i th block. In other words the downlink transmitter is ignoring the fact that $\mathbf{H}_i \neq \mathbf{H}_{i-1}$. In Figure 3.5, we present the average rate per user versus the temporal channel correlation k in (3.18). From these results we note very high sensitivity of the schemes to the channel mismatch. In this particular case the performance of the ZF and MZF schemes becomes worse than when there is no pre-filtering. Note that the above example and the model in (3.18) is a simplification that we use only to illustrate the schemes' sensitivity to imperfect knowledge of the channel state. In the following section we introduce a detailed channel model incorporating spatial and temporal characteristics.

3.2 Channel Model

In the following we first address the spatial aspects of the channel \mathbf{H} . For each mobile terminal there is a $1 \times M$ dimensional channel between its receive antenna and the M transmit antennas at the base station. The MISO channel $\mathbf{h}_n = [h_{n1} \dots h_{nM}]$ for mobile terminal n ($n = 1, \dots, N$) corresponds to the n th row of the channel matrix \mathbf{H} , and we assume that it is independent from other channels (i.e., rows of the channel matrix).

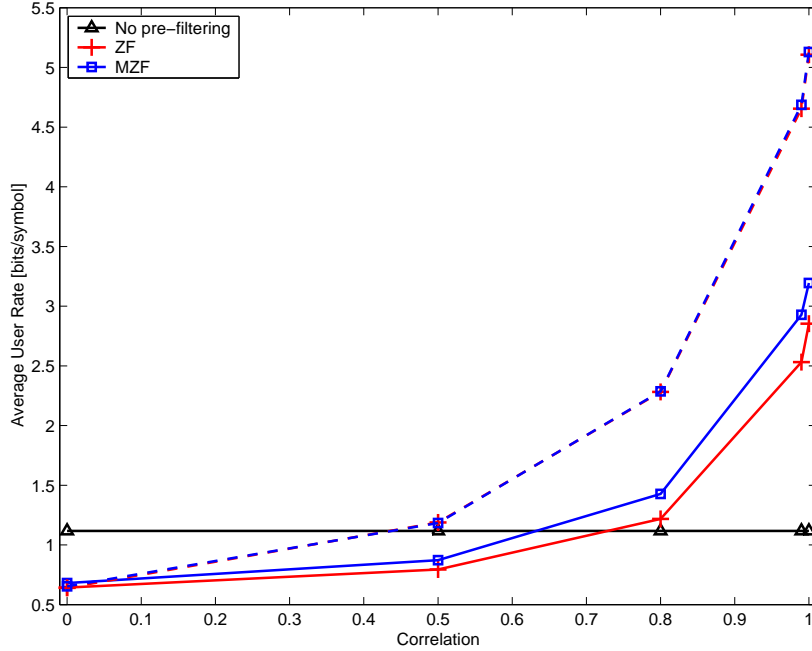


Figure 3.5: Average rate per user vs. temporal channel correlation k , $SNR = 10\text{dB}$, $M = 3$ (solid lines), $M = 6$ (dashed lines), $N = 3$, Rayleigh channel.

Constraining the analysis to two dimensional (2D) space, the n th MISO channel is $\mathbf{h}_n = [h_n(\mathbf{r}_1) \cdots h_n(\mathbf{r}_M)]$, where \mathbf{r}_m is the position of the transmit antenna m in the 2D plane. The channel response $h_n(\mathbf{r}_m)$ between transmit antenna m and the receive antenna of mobile terminal n , is given as a superposition of plane waves

$$h_n(\mathbf{r}_m) = \int_{-\pi}^{\pi} A(\alpha) e^{-j\mathbf{k} \cdot \mathbf{r}_m} d\alpha \quad (3.19)$$

where $\mathbf{k} = [\frac{2\pi}{\lambda} \cos(\alpha + \alpha_n) \quad \frac{2\pi}{\lambda} \sin(\alpha + \alpha_n)]$ is the wave vector of a 2D plane wave in the direction corresponding to the angle $\alpha + \alpha_n$. Note that α_n corresponds to the angle of the mobile terminal boresight and it is an instantiation of a real random variable distributed uniformly over the interval $[0 \ 2\pi]$. λ is the wavelength of the plane wave. Furthermore, $A(\alpha)$ is a complex plane wave arriving at the base station antenna from the angle α relative to α_n . In other words, the channel response $h_n(\mathbf{r}_m)$ in (3.19) is an infinite sum (integral) of all plane waves at the location \mathbf{r}_m . Further, it is assumed here that $A(\alpha)$ has the following statistical property

$$\mathbb{E}[A(\alpha)A(\beta)^*] = P(\alpha)\delta(\alpha - \beta) \quad (3.20)$$

where $P(\alpha)$ is the angular power density of the electromagnetic radiation at the base station. $P(\alpha)$ is also referred to as the power azimuth spectrum [63]. The *rms* angular (i.e., azimuth) spread [64] is defined as

$$AS = \sqrt{\int_{-\pi}^{\pi} \alpha^2 P(\alpha) d\alpha}. \quad (3.21)$$

For cellular systems, where the relevant scatterers are more likely to be close to the mobile terminal, $P(\alpha)$ is typically modeled as a Gaussian distribution shaped function [64]

$$P(\alpha) = \frac{\kappa}{\sqrt{2\pi}\sigma} e^{-\frac{\alpha^2}{2\sigma^2}} \quad (3.22)$$

where the constant κ is determined from the condition $\int_{-\pi}^{\pi} P(\alpha) d\alpha = 1$. Note that $\sigma \approx AS$ (given in (3.21)) when $\sigma \ll \pi$. Other distributions such as Laplacian have also been used to model the angular power density (see [63, 65]).

The spatial correlation between two channel responses $h_n(\mathbf{r}_i)$ and $h_n(\mathbf{r}_j)$ corresponding to transmit antennas i and j and mobile terminal n is then given by

$$\phi_{ij} = \mathbb{E}[h_n(\mathbf{r}_i)h_n(\mathbf{r}_j)^*] = \int_{-\pi}^{\pi} P(\alpha) e^{-j\mathbf{k}(\mathbf{r}_i - \mathbf{r}_j)} d\alpha. \quad (3.23)$$

For the given $P(\alpha)$ the correlation ϕ_{ij} can be computed numerically from the above expression. The correlation ϕ_{ij} is the i th row and the j th column element of the spatial correlation matrix

$$\mathbf{\Phi}_n = \mathbb{E}[\mathbf{h}_n^H \mathbf{h}_n]. \quad (3.24)$$

To obtain a spatially correlated row vector (i.e., a MISO channel \mathbf{h}_n)

$$\mathbf{h}_n = [n_1 \cdots n_M] \mathbf{\Phi}_n^{1/2} \quad (3.25)$$

where $n_i, i = 1, \dots, M$, are complex *iid* random variables with distribution $\mathcal{N}_{\mathcal{C}}(0, 1)$. In general, channels with lower angular spread have higher degree of spatial correlations. For example, in the extreme case of $\sigma = 0^\circ$, the channel has the highest degree of spatial correlation, resulting in a single eigenvector of the spatial correlation matrix $\mathbf{\Phi}_n$ (i.e., infinitely large condition number of the matrix $\mathbf{\Phi}_n$). On the other hand when the channel is spatially uncorrelated $\mathbf{\Phi}_n = \mathbf{I}_{M \times M}$ and its condition number is 1.

The temporal evolution of the spatially correlated MISO channel \mathbf{h}_n may be represented as [66, 67]

$$\mathbf{h}_n(t) = [1 \cdots 1] \mathbf{D}_n \mathbf{N}_n \mathbf{\Phi}_n^{1/2}, \quad \mathbf{D}_n \in \mathcal{C}^{N_f \times N_f}, \mathbf{N}_n \in \mathcal{C}^{N_f \times M} \quad (3.26)$$

where \mathbf{N}_n is a $N_f \times M$ dimensional matrix with elements corresponding to complex *iid* random variables with distribution $\mathcal{N}_{\mathcal{C}}(0, 1/N_f)$. \mathbf{D}_n is a $N_f \times N_f$ diagonal Doppler shift matrix with diagonal elements

$$d_{ii} = e^{j\omega_i t} \quad (3.27)$$

representing the Doppler shifts that affect N_f plane waves and

$$\omega_i = \frac{2\pi}{\lambda} v_n \cos(\gamma_i), \text{ for } i = 1, \dots, N_f \quad (3.28)$$

where v_n is the velocity of mobile terminal n and the angle of arrival of the i th plane wave at the terminal is γ_i (generated as $\mathcal{U}[0 \ 2\pi]$).

It can be shown that the model in (3.26) strictly conforms to the Jakes model for $N_f \rightarrow \infty$. This model assumes that at the mobile terminal the plane waves are coming from all directions with equal probability. With minor modifications, the above model can be modified to capture non-uniform arrival of the plane waves at the terminal. Further, note that each diagonal element of \mathbf{D}_n corresponds to one Doppler shift. The matrix $\mathbf{N}_n \mathbf{\Phi}_n^{1/2}$ is introducing spatial correlations at the base station for each Doppler shift. For each mobile terminal, \mathbf{D}_n and \mathbf{N}_n are independently generated.

Let us consider the following MISO channel model

$$\mathbf{h}_n(t) = \left(k_n(t) \mathbf{n}_0 + \sqrt{1 - k_n(t)^2} \mathbf{n}_t \right) \mathbf{\Phi}_n^{1/2} \quad (3.29)$$

where $\mathbf{n}_0 = [n_{01} \cdots n_{0M}]$ and $\mathbf{n}_t = [n_{t1} \cdots n_{tM}]$ with the components n_{0i} and n_{ti} ($i = 1, \dots, M$) being complex *iid* random variables with distribution $\mathcal{N}_{\mathcal{C}}(0, 1)$. Assuming the Jakes model, $k_n(t) = J_0(2\pi v_n t / \lambda)$. Considering the time instant 0 and t , it can be shown that the models in (3.26) and (3.29) are statistically equivalent as $N_f \rightarrow \infty$. In both cases the components of the vector $\mathbf{h}_n(t)$ have a zero mean complex Gaussian distribution and have the same covariance $\mathbb{E}[\mathbf{h}_n(t)^H \mathbf{h}_n(t)] = \mathbf{\Phi}_n$ and $\mathbb{E}[\mathbf{h}_n(0)^H \mathbf{h}_n(t)] = k_n(t) \mathbf{\Phi}_n$.

Using the above MISO channel model, the following channel properties relate temporal and spatial characteristics of the channel.

1. The mean squared distance (MSD) between the MISO channel response $\mathbf{h}_n(t)$ and $\mathbf{h}_n(0)$ is a function of time t and does not depend on the spatial correlation of the channel. In other words

$$\text{MSD}_n(t) = \text{E}[|\mathbf{h}_n(t) - \mathbf{h}_n(0)|^2]. \quad (3.30)$$

Since $\text{trace}(\mathbf{\Phi}_n) = M$, it follows that the MSD is

$$\text{MSD}_n(t) = 2M(1 - k_n(t)). \quad (3.31)$$

2. The average power of the MISO channel response $\mathbf{h}_n(t)$ in the direction of $\mathbf{h}_n(0)$ (i.e., the projection of $\mathbf{h}_n(t)$ on $\mathbf{h}_n(0)$)

$$\zeta(t) = \frac{1}{M} \text{E} \left[\left| \frac{\mathbf{h}_n(0)\mathbf{h}_n(t)^H}{\sqrt{\mathbf{h}_n(0)\mathbf{h}_n(0)^H}} \right|^2 \right] \quad (3.32)$$

and it increases with the spatial correlation of the channel. Specifically,

$$\zeta(t) = k_n(t)^2 + (1 - k_n(t)^2) \frac{\sum_{i=1}^M \psi_{ni}^2}{M^2} \quad (3.33)$$

where ψ_{ni} ($i = 1, \dots, M$) are eigenvalues of the matrix $\mathbf{\Phi}_n$. Figure 3.6 presents $\zeta(t)$ for different spatial correlations of the channel and also a spatially uncorrelated channel (based on the model in (3.26), $f_c = 2\text{GHz}$, $v = 30\text{kmph}$). The results indicate that $\zeta(t)$ is increasing with the spatial correlation (as said earlier, low values of σ correspond to high spatial correlations).

Numerical Results

In Figure 3.7 and 3.8 we present average rates per user versus the delay τ of the CSI. The system consists of $M = 3$ transmit antennas and $N = 3$ terminals. The channel is modeled based on (3.26) (assuming that the carrier frequency is 2GHz and the velocity of each mobile terminal is 30kmph and setting the number of plane waves $N_f = 100$). We assume that the transmit antennas form a proper phased array being spaced $\lambda/2$

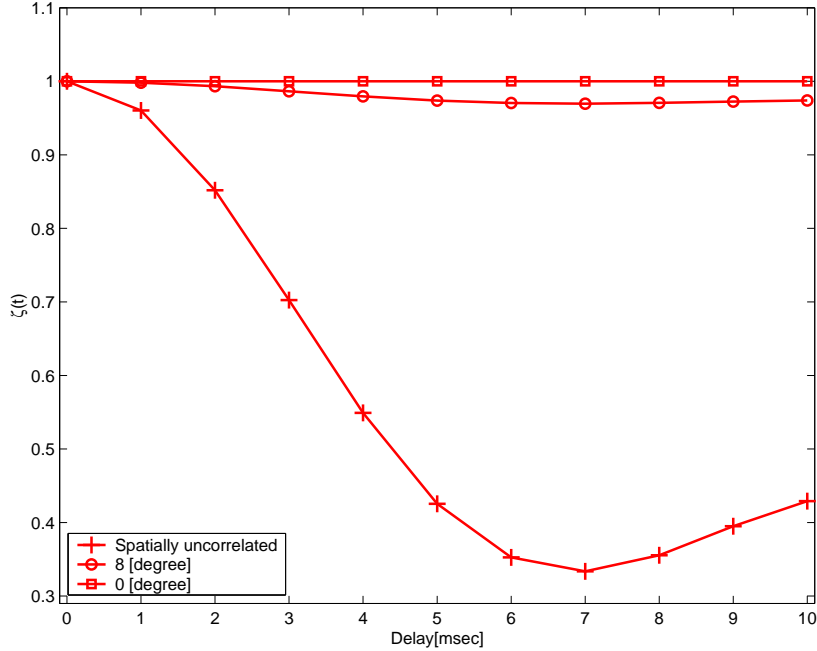


Figure 3.6: $\zeta(t)$ for $M = 3$ and channel based on model in (3.26), $f_c = 2\text{GHz}$, $v = 30\text{kmph}$.

apart. Because the ideal channel state $\mathbf{H}(t + \tau)$ is not available at the transmitter, we assume that $\mathbf{H}(t)$ is used instead to perform the transmitter optimization at the moment $t + \tau$. We observe performance for different spatial correlations of the channel and for the spatially uncorrelated channel. Figures 3.7 and 3.8 present average rates for the ZF and MZF scheme respectively, for $SNR = 10\text{dB}$. In all cases, we observe that as the CSI delay increases, spatially uncorrelated channels perform worse than spatially correlated channels, which is a result in contrast to the case of zero delay CSI. In the extreme case of $\sigma = 0^\circ$, the average rate is hardly affected by the delay of the CSI, while for the spatially uncorrelated channels degradation due to the delay is significant.

In the following we outline the explanation of the above results using a subspace decomposition of the matrix \mathbf{H} . Let $\tilde{\mathcal{C}}_n(t)$ for user n denote the subspace spanned by the row vectors of the channel matrix \mathbf{H} other than the n th row. Let us further define the matrix $\mathbf{B}_n(t)$ ($\mathbf{B}_n(t) \in \mathcal{C}^{N-1 \times M}$) such that its row vectors correspond to the orthonormal basis that spans $\tilde{\mathcal{C}}_n(t)$. We observe the expected valued of the normalized

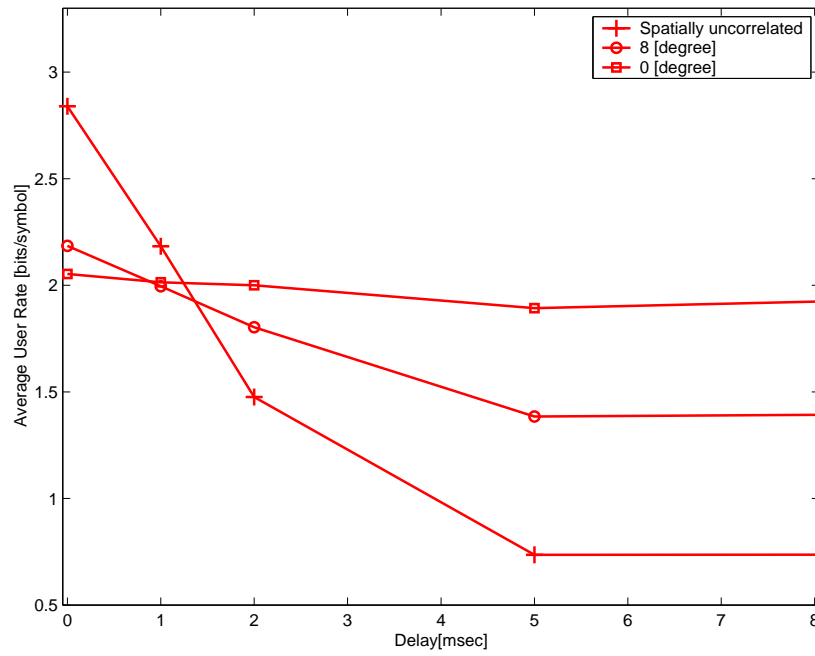


Figure 3.7: The ZF scheme, average rate per user vs. CSI delay, $SNR = 10\text{dB}$, $M = 3$, $N = 3$, channel based on model in (3.26), $f_c = 2\text{GHz}$, $v = 30\text{kmph}$.

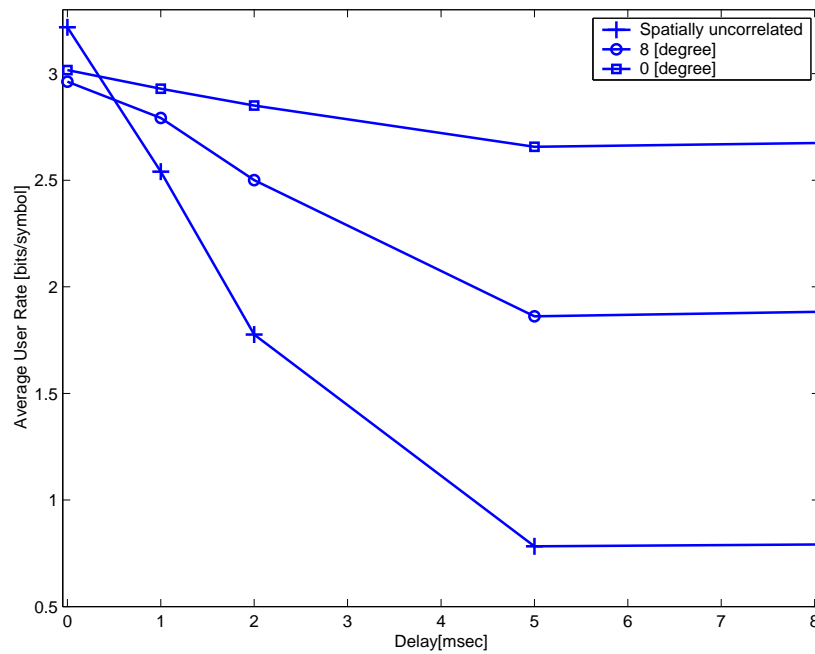


Figure 3.8: The MZF scheme, average rate per user vs. CSI delay, $SNR = 10\text{dB}$, $M = 3$, $N = 3$, channel based on model in (3.26), $f_c = 2\text{GHz}$, $v = 30\text{kmph}$.

Frobenius norm ($\|\cdot\|^2$) of the product of the basis vectors at the instance t and $t + \tau$

$$\rho_n(\tau) = \frac{\mathbb{E} \left[\left\| \mathbf{B}_n(t + \tau) \mathbf{B}_n(t)^H \right\|^2 \right]}{N - 1}. \quad (3.34)$$

Figure 3.9 presents $\rho_n(\tau)$ for different spatial correlations of the channel and also a spatially uncorrelated channel. Note that it can be shown that in the static case $\rho_n(\tau) = 1$, while for the case of fully independent $\mathbf{H}(t)$ and $\mathbf{H}(t + \tau)$, $\rho_n(\tau) = (N - 1)/M$. These two values represent the upper and lower bound of $\rho_n(\tau)$, respectively. Based on Figure 3.9, with respect to the temporal variations of the subspace $\tilde{\mathcal{C}}_n(t)$, the case of $\sigma = 0$ is equivalent to the static case (having the upper bound of $\rho_n(\tau)$ for all τ). Furthermore, the spatially uncorrelated channel is approaching the case of independent $\mathbf{H}(t)$ and $\mathbf{H}(t + \tau)$ for large τ (approaching the lower bound of $\rho_n(\tau)$).

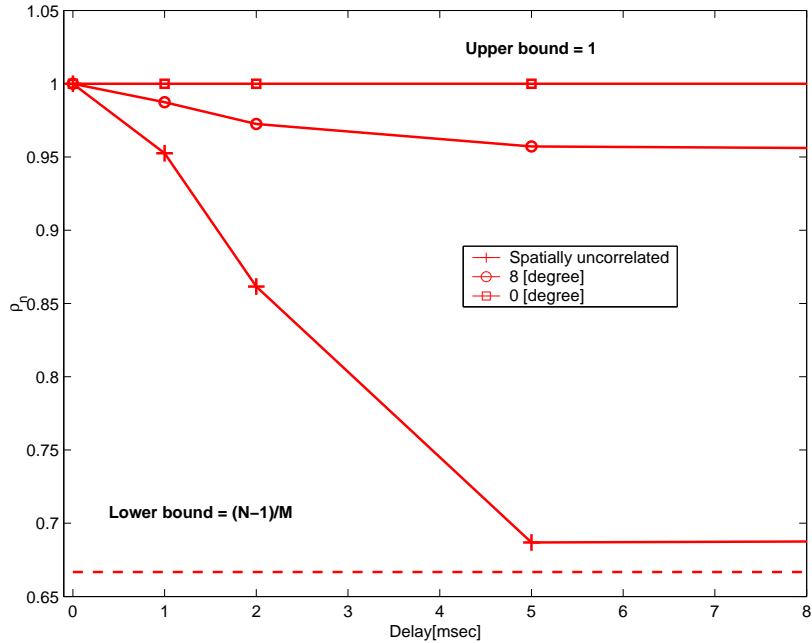


Figure 3.9: $\rho_n(\tau)$ for $M = 3$, $N = 3$ and channel based on model in (3.26), $f_c = 2\text{GHz}$, $v = 30\text{kmph}$.

What this shows is that under the case of strong spatial correlations, the subspace $\tilde{\mathcal{C}}_n(t)$ is relatively stable (i.e., changing slowly in time). As a result, any transmitter optimization (pre-filtering) scheme is relatively robust to temporal delays in the CSI feedback. For the case of spatially uncorrelated channels, this robustness is lost leading

to poorer performance of transmitter optimization.

3.3 Channel State Prediction

Let us assume that the transmitter has a set of previous channel responses (for mobile terminal n) $\mathbf{h}_n(t)$ where $t = kT_{ch}$ and $k = 0, -1, \dots, -(L-1)$. The time interval T_{ch} may correspond to a period when a new CSI is sent from the mobile terminal to the base station. Knowing that the wireless channel has temporal and spatial correlations, based on previous channel responses the transmitter may perform a prediction of the channel response $\mathbf{h}_n(\tau)$ at the time moment τ . In this study we assume that the prediction is linear and that it minimizes the mean squared error (MMSE) between true and predicted channel state. The MMSE predictor \mathbf{W}_n is

$$\mathbf{W}_n = \arg_{\mathbf{T}} \min \mathbb{E} |\mathbf{T}^H \mathbf{h}_{un} - \mathbf{h}_n(\tau)|^2 \quad (3.35)$$

where \mathbf{h}_{un} is an *uber* vector defined as

$$\mathbf{h}_{un} = [\mathbf{h}_n(0) \ \mathbf{h}_n(-T_{ch}) \ \dots \ \mathbf{h}_n(-(L-1)T_{ch})]^T. \quad (3.36)$$

In other words, the *uber* vector is constructed by stacking up the previous channel responses available to the transmitter. Let us define the following matrices

$$\mathbf{U}_n = \mathbb{E} [\mathbf{h}_{un} \mathbf{h}_{un}^H] \quad (3.37)$$

and

$$\mathbf{V}_n = \mathbb{E} [\mathbf{h}_{un} \mathbf{h}_n(\tau)]. \quad (3.38)$$

It can be shown that the linear MMSE predictor \mathbf{W}_n is [68]

$$\mathbf{W}_n = \mathbf{U}_n^{-1} \mathbf{V}_n. \quad (3.39)$$

The above predictor exploits both temporal and spatial correlations of the MISO channel. Note that different linear predictors are needed for different mobile terminals.

A practical implementation of the above prediction can use sample estimates of \mathbf{U}_n and \mathbf{V}_n as

$$\hat{\mathbf{U}}_n = \frac{1}{N_w} \sum_{i=-N_w}^{-1} \mathbf{h}_{un}(iT_{ch}) \mathbf{h}_{un}(iT_{ch})^H \quad (3.40)$$

$$\hat{\mathbf{V}}_n = \frac{1}{N_w} \sum_{i=-N_w}^{-1} \mathbf{h}_{un}(iT_{ch})\mathbf{h}_n(\tau + iT_{ch}). \quad (3.41)$$

The underlying assumption in using the above estimates is that the channel is stationary over the integration window $N_w T_{ch}$. Further, if the update of the CSI is performed at discrete time moments kT_{ch} ($k = 0, -1, \dots$), the update period T_{ch} should be such that

$$T_{ch} < \frac{1}{2f_{doppler}}. \quad (3.42)$$

Numerical Results

In Figure 3.10 we present the normalized mean square error between assumed and true channel state versus the CSI delay τ (assuming that the carrier frequency is 2GHz and the velocity of each mobile terminal is 30kmph and $N_f = 100$). The normalized error is computed using the Frobenius norm for both the case of no prediction and MMSE prediction. The solid lines correspond to $E\|\mathbf{H}(t+\tau) - \mathbf{H}(t)\|^2/E\|\mathbf{H}(t+\tau)\|^2$ (case without the MMSE prediction) while dashed lines correspond to $E\|\mathbf{H}(t+\tau) - \mathbf{H}_{mmse}(t+\tau)\|^2/E\|\mathbf{H}(t+\tau)\|^2$ (case with the MMSE prediction) where $\mathbf{H}_{mmse}(t+\tau)$ denotes the predicted channel state. We set $T_{ch} = \tau$, corresponding to the worst case delay. The results are presented for channels with different spatial correlations. Note that in the case when no prediction is applied, the normalized error is the same for any degree of spatial correlations and Figure 2.8 shows three curves (corresponding to $\sigma = 0^\circ$, $\sigma = 8^\circ$ and spatially uncorrelated) all laying on each other. This result conforms to the property in (3.31). Further we note that the MMSE prediction greatly improves the quality of the assumed channel state. As expected, we also note that channels with higher degrees of spatial correlation result in lower normalized mean square error when the prediction is applied. Beyond a certain value of the CSI delay τ , the MMSE prediction performs equally well for channels with high and low spatial correlations.

Using the same system assumptions as in Figure 3.7 and 3.8, in Figure 3.11 and 3.12 we present average rates per user versus the delay τ of the CSI. Results depicted by the solid lines correspond to the application of the delayed CSI $\mathbf{H}(t)$ instead of the true channel state $\mathbf{H}(t+\tau)$. The dashed lines depict results when the MMSE

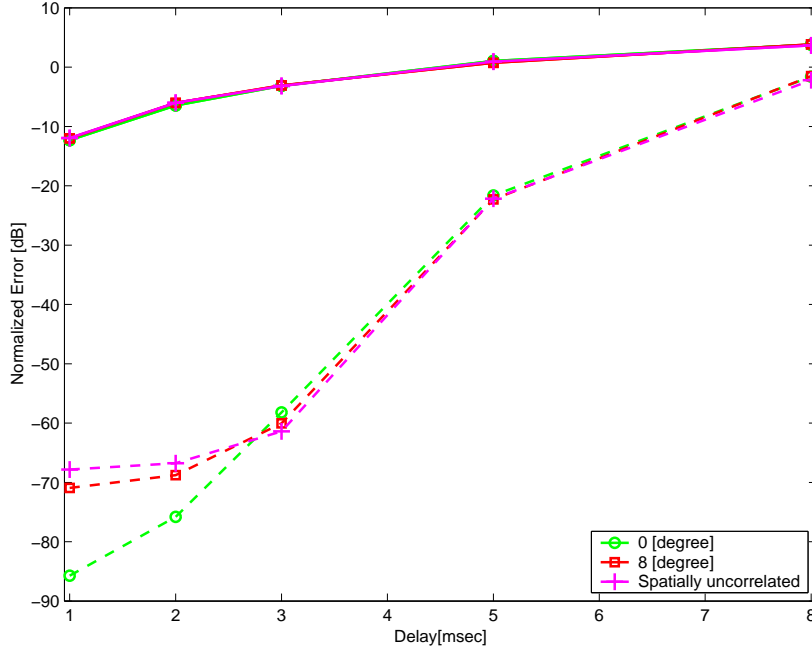


Figure 3.10: Normalized mean squared error between assumed and true channel state vs. CSI delay, with MMSE prediction (dashed lines) and without MMSE prediction (solid lines), $M = 3$, $N = 3$, channel based on model in (3.26), $f_c = 2\text{GHz}$, $v = 30\text{kmph}$.

predicted channel state $\mathbf{H}_{mmse}(t + \tau)$ is used instead of the true channel state $\mathbf{H}(t + \tau)$. Without any particular effort to optimally select the implementation parameters, in this particular example, we use $L = 10$ previous channel responses to construct the *uber* vectors in (3.36). Further, the length of the integration window in (3.40) and (3.41) is selected to be $N_w = 100$. The results in Figure 3.11 and 3.12 clearly point to improvements in the performance of the schemes when the MMSE channel state prediction is used. The MMSE prediction scheme is seen to improve the performance of spatially uncorrelated channels in terms of the maximum CSI delay before which it deteriorates in comparison to the spatially correlated case. Note that the improvements are comparable both in the case of low and high spatial correlations. The results suggest that the temporal correlations in the channel alone are significant enough to support the application of the MMSE prediction.

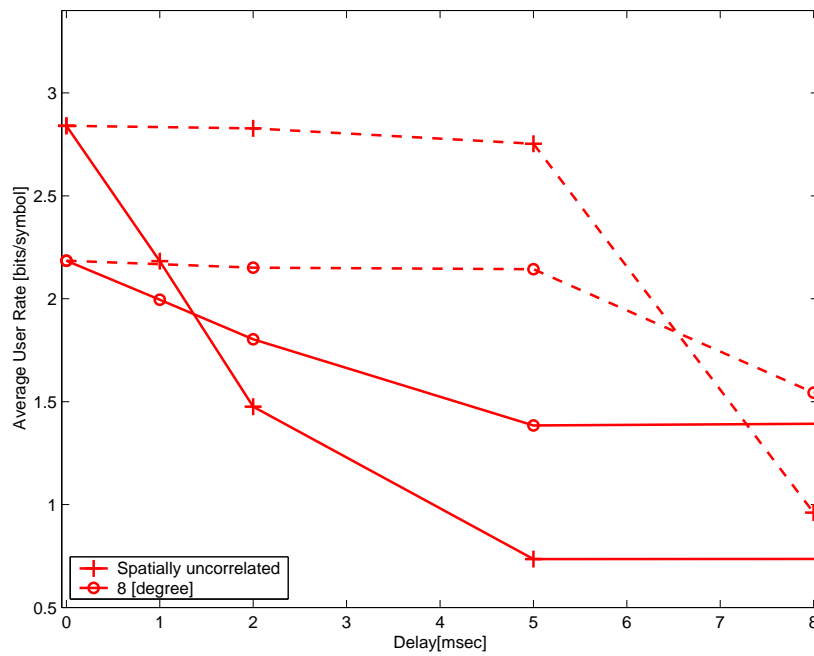


Figure 3.11: The ZF scheme, average rate per user vs. CSI delay, with MMSE prediction (dashed lines) and without MMSE prediction (solid lines), $SNR = 10\text{dB}$, $M = 3$, $N = 3$, channel based on model in (3.26), $f_c = 2\text{GHz}$, $v = 30\text{kmph}$.

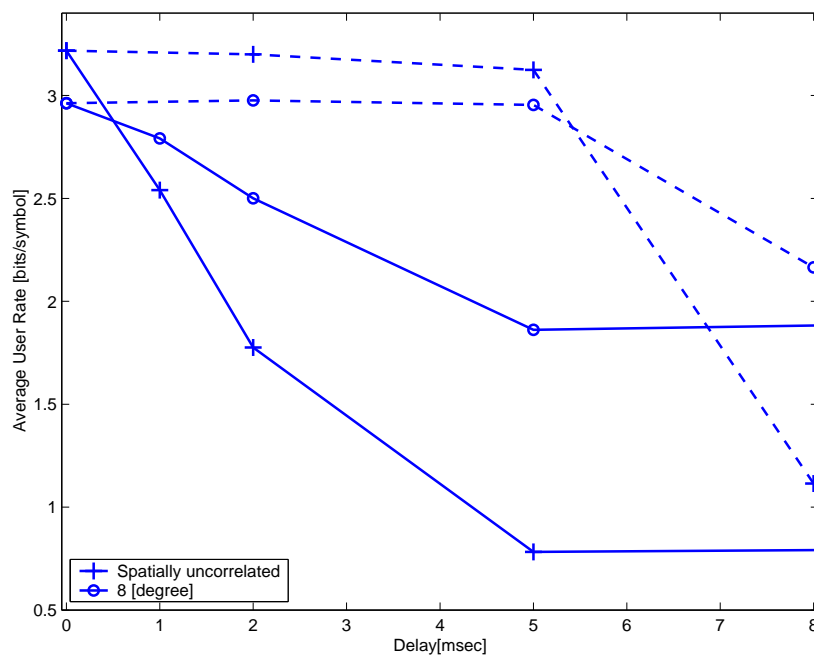


Figure 3.12: The MZF scheme, average rate per user vs. CSI delay, with MMSE prediction (dashed lines) and without MMSE prediction (solid lines), $SNR = 10\text{dB}$, $M = 3$, $N = 3$, channel based on model in (3.26), $f_c = 2\text{GHz}$, $v = 30\text{kmph}$.

3.4 Conclusion

In this Chapter we have presented a study on multiple antenna transmitter optimization schemes that are based on linear transformations and transmit power optimization. We have shown that the triangularization with DPC approaches the closed loop MIMO rates (upper bound) for higher SNR. Further, the MZF solution performs very well for lower SNRs (approaching CL-MIMO and DPC rates), while for higher SNRs the rates for the ZF scheme converge to the MZF rates. In addition, we have presented how the average rates depend on number of transmit antennas, while keeping the number of terminals constant. With the number of transmit antennas increasing the rates increase, and the difference between the rates for different schemes gets smaller. Further, we have studied the performance of the transmitter optimization schemes with respect to the delayed CSI. It was seen that as the CSI delay increases, spatially uncorrelated channels perform worse than spatially correlated channels, which is in contrast to the case of zero delay CSI. A linear MMSE predictor of the channel state was also introduced which improved the performance in all cases. Further, we have shown that the predictor increases the tolerable maximum CSI delay for which the performance on spatially uncorrelated channels is higher than that of the correlated case. The results have suggested that the temporal correlations in the channel alone are significant enough to support the application of the MMSE prediction.

Chapter 4

Unquantized and Uncoded Channel State Information Feedback on Wireless Channels

In this chapter we consider a system where a mobile terminal obtains the downlink CSI and feeds it back to the base station using an uplink feedback channel. If the downlink channel is an independent Rayleigh fading channel, then the CSI may be viewed as an output of a complex independent identically distributed (*iid*) Gaussian source. Further if the uplink feedback channel is AWGN, it can be shown that unquantized and uncoded (UQ-UC) CSI transmission (that incurs zero delay) is optimal in that it achieves the same minimum mean squared error (MMSE) distortion as a scheme that optimally (in the Shannon sense) quantizes and encodes the CSI while incurring infinite delay [42]. Results on the optimality of unquantized and uncoded transmission have also been discussed in other contexts in [69–71]. Since the UQ-UC transmission is suboptimal on correlated wireless channels, we propose a simple linear CSI feedback receiver that can be used in conjunction with the UQ-UC transmission while still retaining the attractive zero-delay feature. Furthermore, we describe an auto regressive-moving average (ARMA) correlated channel model and present the corresponding performance bounds for the UQ-UC CSI feedback scheme. We explore the performance limits of such schemes in the context of multiple antenna multiuser wireless systems [42].

4.1 Background

Consider the communication system in Figure 4.1. The system is used for transmission of unquantized and uncoded outputs (i.e., symbols) of the source. The source is complex, continuous in amplitude and discrete in time (with the symbol period T_{sym}). We assume that the symbols x are zero-mean with unit variance. The average transmit

power is P , while the channel introduces additive zero-mean noise n with variance N_0 . At the receiver, the received signal y is multiplied by the conjugate of w . Consequently, the signal \hat{x} at the destination is

$$\hat{x} = w^*y = w^* (\sqrt{P}x + n) \quad (4.1)$$

and \hat{x} is an estimate of the transmitted symbol x . We select the coefficient w to minimize the mean squared error (MSE) between \hat{x} and x . Thus,

$$w = \arg \min E|\hat{x} - x|^2 = \arg_v \min E|v^* (\sqrt{P}x + n) - x|^2. \quad (4.2)$$

Consequently,

$$w = \frac{\sqrt{P}}{P + N_0} \quad (4.3)$$

and the corresponding mean squared error is

$$\min E|\hat{x} - x|^2 = \frac{1}{1 + \frac{P}{N_0}}. \quad (4.4)$$

The MSE corresponds to a measure of distortion between the source symbols and estimates at the destination.

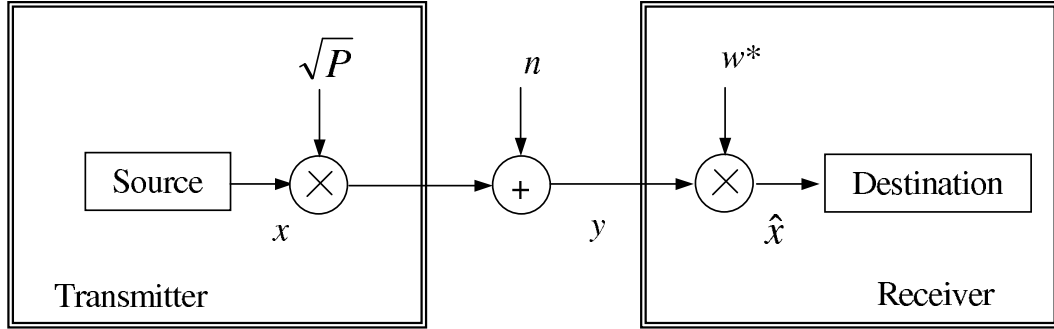


Figure 4.1: Unquantized and uncoded transmission that achieves the MMSE distortion of the transmitted signal.

Let us now relate the above results to the transmission scheme that applies optimal quantization and channel coding. Based on the Shannon rate distortion theory [57], for a given distortion D^* , the average number of bits per symbol at the output of the optimal quantizer is

$$R = \log_2 \left(1 + \frac{1 - D^*}{D^*} \right). \quad (4.5)$$

Note that the optimal quantizer that achieves the above rate incurs infinite quantization delay. For the AWGN channel, the maximum transmission rate is

$$C = \log_2 \left(1 + \frac{P}{N_0} \right). \quad (4.6)$$

As in the case of the optimal quantizer, the optimal channel coding would incur infinite coding delay. Furthermore, optimal matching (in the Shannon sense) of the quantizer and the channel requires that

$$R = C \Rightarrow D^* = 2^{-C} = \frac{1}{1 + \frac{P}{N_0}}. \quad (4.7)$$

The above distortion is equal to the MSE for the UQ-UC transmission scheme given in (4.4) (see also [70]). The above result points to the optimality of the UQ-UC scheme (while it incurs zero delay) when the source is *iid* Gaussian and the channel is AWGN.

4.2 UQ-UC CSI Feedback

Using the above result, we now motivate why UQ-UC transmission schemes can be used for CSI feedback in wireless systems. Consider the communication system shown in Figure 4.2. It consists of a base station transmitting data over a downlink channel. A mobile terminal receives the data, and transmits the CSI of the downlink channel state h_{dl} over an uplink channel. Let us assume that the mobile terminal estimates the downlink CSI h_{dl} perfectly. If the downlink channel is *iid* Rayleigh, then the CSI is an *iid* complex Gaussian random variable. In this case, if the uplink channel is AWGN and it is independent of the downlink channel, then it follows directly from the earlier discussion that the above UQ-UC scheme is optimal for transmission of the downlink CSI over the uplink channel. In other words, for the communication system shown in Figure 4.2, UQ-UC transmission (with zero delay) of the downlink CSI will achieve the same distortion as a scheme that optimally (in the Shannon sense) quantizes and encodes the CSI while incurring infinite delay.

To further distinguish the fact that the UQ-UC CSI feedback transmission does not imply an "analog" communication¹ system, we now illustrate an example of how such a

¹While we use the term unquantized (UQ) in the UQ-UC nomenclature, it must be pointed out that any practical transmission scheme will require at least some level of coarse quantization.

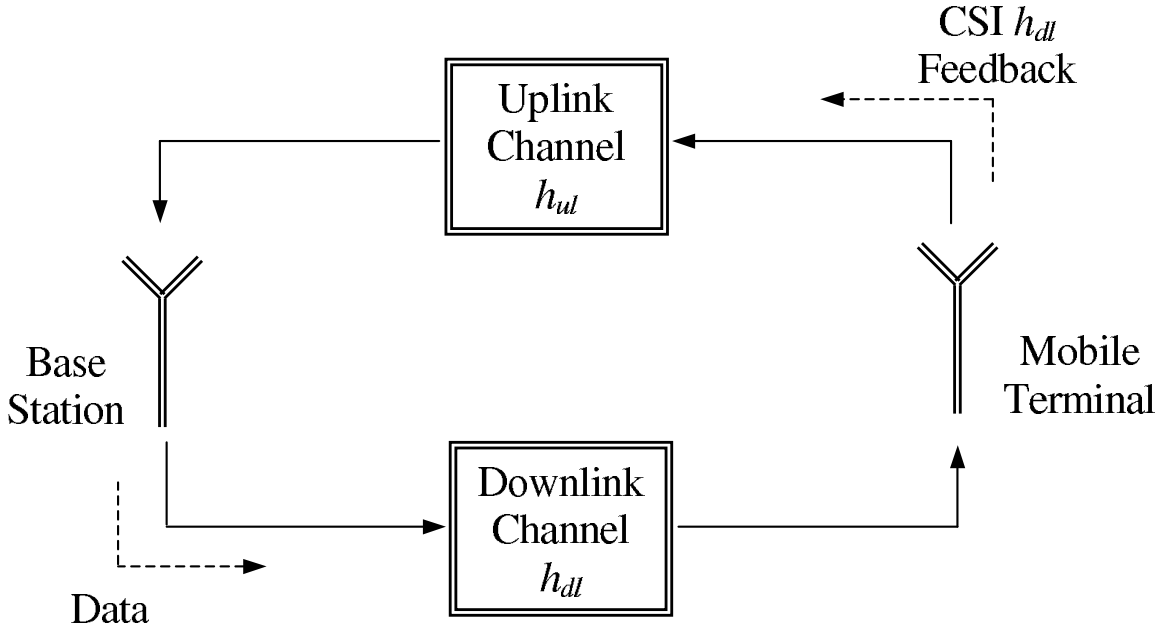


Figure 4.2: Communication system with CSI feedback.

scheme could be applied in the context of a CDMA system. The functional blocks of the mobile terminal in a CDMA system are depicted in Figure 4.3. Using a pilot assisted estimation scheme, the mobile terminal obtains an estimate of the downlink channel h_{dl} , denoted as \bar{h}_{dl} . The downlink channel estimate \bar{h}_{dl} is the CSI to be transmitted on the uplink channel h_{ul} . The estimate \bar{h}_{dl} modulates (i.e., multiplies) a Walsh code that is specifically allocated as a CSI feedback carrier as shown in Figure 4.3. The second Walsh code is allocated for the conventional uplink data transmission. For generality, the uplink pilot is also transmitted allowing the base station to obtain an estimate \bar{h}_{ul} of the uplink channel h_{ul} .

4.3 UQ-UC CSI Feedback on Correlated Channels

The MSE distortion achieved by the UQ-UC CSI feedback transmission scheme is optimal when the downlink is *iid* Rayleigh and the uplink is AWGN, and further, the uplink and the downlink are also mutually independent. In reality, there may be the following situations that arise in wireless systems: (1) temporal correlations in the downlink channel, (2) temporal correlations in the uplink channel, and (3) correlations between the

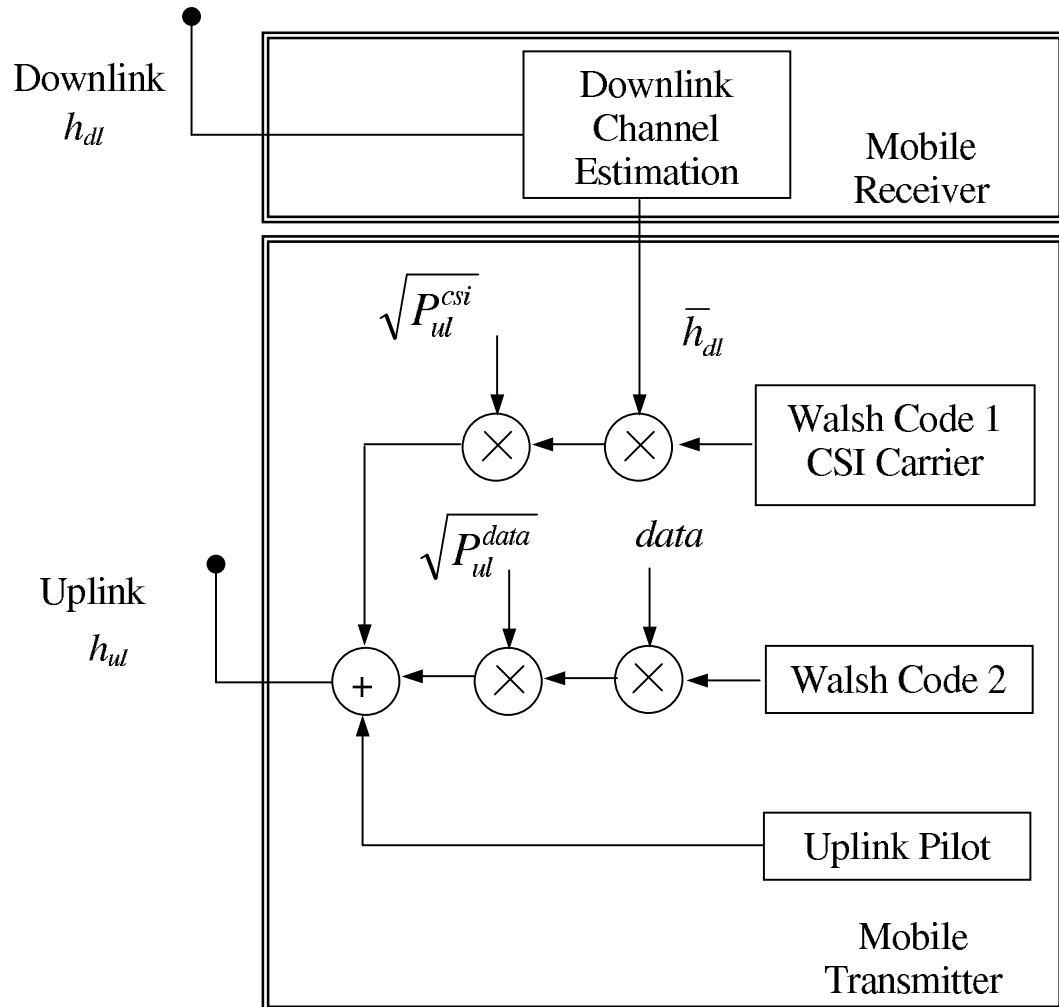


Figure 4.3: CDMA mobile terminal that applies the UQ-UC CSI feedback.

uplink and the downlink channels (as is in TDD systems). In each of these cases, it is of interest to quantify the MSE distortion achieved by the UQ-UC CSI feedback. Since, an exact analysis is not readily tractable, we propose to quantify such performance through upper and lower bounds in each of the above scenarios.

4.3.1 Performance Bounds

Let us assume the uplink and downlink channel states are independent (which is typical in FDD wireless systems). Both the uplink and downlink channels are varying in time and are assumed to be ergodic. If the scheme shown in Figure 4.1 is now applied on the CSI feedback channel (explicitly accounting for the uplink channel state h_{ul}), then it follows that the MSE is

$$MSE_{uq-uc}^{ub} = E_{h_{ul}} \left[\frac{1}{1 + \frac{|h_{ul}|^2 P_{ul}^{csi}}{N_0}} \right]. \quad (4.8)$$

Clearly this serves as an upper bound on the MSE achieved by any additional processing that accounts for both the downlink and the uplink CSI feedback channel being correlated channels.

To illustrate an approach to derive a lower bound, consider an L th order autoregressive-moving average (ARMA) process model for the downlink channel as

$$h_{dl}(i) = \sum_{j=1}^L c_j h_{dl}(i-j) + c_0 n_{dl}(i), \quad (4.9)$$

where $n_{dl}(i)$ is a complex Gaussian random variable with distribution $\mathcal{N}_{\mathcal{C}}(0,1)$. The coefficients c_j ($j = 0, \dots, L$) determine the correlation properties of the channel. $n_{dl}(i)$ is the innovation sequence that describes the evolution to successive channel states. The above model gives a general framework for describing the correlations in the downlink channel states through the coefficients c_j ($j = 0, \dots, L$). Furthermore, using an approach outlined in [42] and Appendix C, it is possible to explicitly approximate the well known the Jakes correlated fading model by relating parameters such as carrier frequency and mobile speed to the ARMA model coefficients and the channel update interval.

Let us assume that the above model and the previous channel states $h_{dl}(i-j)$ ($j = 1, \dots, L$) are known at the CSI feedback transmitter and receiver. In this idealized case, having only the innovation $n_{dl}(i)$ transmitted over the uplink CSI feedback channel, the receiver can estimate the channel state $h_{dl}(i)$. Similar to the arguments related to equations (4.5) - (4.7), the optimal quantization and channel coding of the innovation $n_{dl}(i)$ results in its MSE

$$\mathbb{E}|\hat{n}_{dl}(i) - n_{dl}(i)|^2 = 2^{-\bar{C}_{ul}}, \quad (4.10)$$

where $\hat{n}_{dl}(i)$ is an estimate of $n_{dl}(i)$ at the receiver and \bar{C}_{ul} is the ergodic capacity of the uplink channel given as

$$\bar{C}_{ul} = \mathbb{E}_{h_{ul}} \left[\log_2 \left(1 + \frac{|h_{ul}|^2 P_{ul}^{csi}}{N_0} \right) \right]. \quad (4.11)$$

Based on (4.9) and (4.10), it can be shown that the MSE of $h_{dl}(i)$ is lower bounded as

$$\mathbb{E}|\hat{h}_{dl}(i) - h_{dl}(i)|^2 \geq c_0^2 2^{-\bar{C}_{ul}}. \quad (4.12)$$

Since this bound is obtained using idealized knowledge of the previous channel states and also a channel coding scheme that achieves the ergodic capacity of the uplink channel, we expect it to be loose. However, the procedure outlined above leads us to believe that it is possible to obtain not only tighter bounds but also bounds for channels beyond the scenario outlined above, i.e., ergodic and mutually independent uplink and downlink channels where the downlink obeys the model in (4.9).

4.3.2 Feedback Receivers for Enhancing UQ-UC CSI Feedback Schemes

While the previous section considered the performance limits of the MSE distortion achieved by the UQ-UC CSI feedback transmission, in this section we will outline signal processing techniques that could be used to improve the performance of UQ-UC schemes. The specific approach that we propose is to design receivers on the CSI feedback channel that can exploit the channel correlations and thus improve the performance in cases where the UQ-UC CSI feedback transmission is suboptimal. We illustrate such an approach through the design of a linear CSI feedback receiver in the following.

Consider a signal/system model, where at the time instant i , the uplink received signal corresponding to the CSI feedback is

$$\mathbf{y}(i) = h_{ul}(i)\bar{h}_{dl}(i) + n(i) \quad (4.13)$$

where $h_{ul}(i)$ is the uplink channel state, $\bar{h}_{dl}(i)$ is the estimate of the downlink CSI that is being fed back and $n(i)$ is the AWGN on the uplink. For simplicity in illustration, let us assume in the following that the estimate $\bar{h}_{dl}(i)$ is perfect, i.e., $\bar{h}_{dl}(i) = h_{dl}(i)$. Using the received signal in (4.13) and an estimate of $\bar{h}_{ul}(i)$, the CSI feedback receiver at the base station will estimate the transmitted CSI $h_{dl}(i)$. Now the question that remains is how to design such a feedback receiver?

Consider a linear CSI feedback receiver that can exploit the correlation structure in the following way. The uplink received signal in (4.13) is used to form a temporal K -dimensional received vector as

$$\mathbf{y}(i) = [y(i) \ y(i-1) \ \cdots \ y(i-K+1)]^T. \quad (4.14)$$

The uplink receiver then estimates the downlink CSI $h_{dl}(i)$ as

$$\hat{h}_{dl}(i) = \mathbf{w}^H \mathbf{y}(i) \quad (4.15)$$

where \mathbf{w} is a linear filter that is derived from the following MMSE optimization

$$\mathbf{w} = \arg_{\mathbf{v}} \min E |\mathbf{v}^H \mathbf{y}(i) - h_{dl}(i)|^2. \quad (4.16)$$

For the given estimates of the uplink channel $\bar{\mathbf{h}}_{ul}(i) = [\bar{h}_{ul}(i) \ \bar{h}_{ul}(i-1) \ \cdots \ \bar{h}_{ul}(i-K+1)]^T$ we define the following matrix

$$\mathbf{U} = E_{\mathbf{y}|\bar{\mathbf{h}}_{ul}} [\mathbf{y} \mathbf{y}^H] \quad (4.17)$$

and the vector

$$\mathbf{s} = E_{h_{dl}, \mathbf{y}|\bar{\mathbf{h}}_{ul}} [h_{dl}^* \mathbf{y}]. \quad (4.18)$$

In the above, we have omitted the temporal index i since we assume a stationary system (i.e., the uplink channel, downlink channel and the AWGN are assumed to be stationary

random processes). It can be shown that the linear MMSE CSI feedback receiver \mathbf{w} is given as

$$\mathbf{w} = \mathbf{U}^{-1}\mathbf{s}. \quad (4.19)$$

As is evident from the equations (4.17)-(4.19), the linear transformation \mathbf{w} takes into account implicitly the following correlations: (1) temporal correlations in the downlink channel, (2) temporal correlations in the uplink channel and (3) the correlations between the uplink and the downlink (as is in TDD systems). In fact, when $K = 1$ and the uplink and the downlink are mutually independent, then the above receiver will achieve the MSE distortion upper bound in equation (4.8). In all other cases, the performance will be superior, thereby enhancing the performance of the UQ-UC CSI feedback transmission.

4.3.3 Numerical Results: Distortion Performance

We consider the case when the uplink and the downlink channels are mutually independent. Further, the downlink channel is modeled as an ARMA process whose coefficients are chosen to correspond to the Jakes model for a carrier frequency of 2GHz and a mobile terminal velocity of 10kmph. For the uplink, we assume that the channel is Rayleigh with an average $SNR_{ul}^{csi} = 10 \log (P_{ul}^{csi}/N_0) = 10\text{dB}$. In Figure 4.4 we show the MSE of the UQ-UC scheme with the linear CSI feedback receiver as a function of the CSI update period τ , where τ is the absolute time difference between successive channel states $h_{dl}(i)$ and $h_{dl}(i-1)$. The corresponding lower and upper bounds are also shown. Figure 4.5 shows the MSE of the same scheme as a function of the CSI update period τ for different mobile terminal velocities. These results show that the linear receiver (for $K = L + 1$) in combination with the UQ-UC transmission is able to exploit the temporal correlations in the channel and improve the performance relative to the lower bound. Note that when either the mobile terminal velocities are low or the CSI update period is small, the improvement is greater.

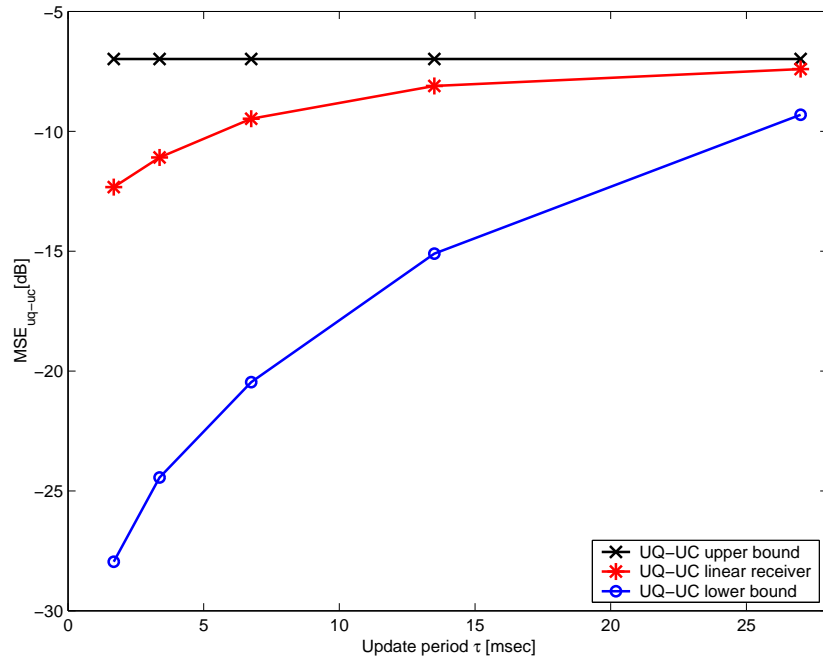


Figure 4.4: MSE vs. CSI update period, $f_c = 2\text{GHz}$, $v = 10\text{kmph}$, average $SNR_{ul}^{csi} = 10\text{dB}$.

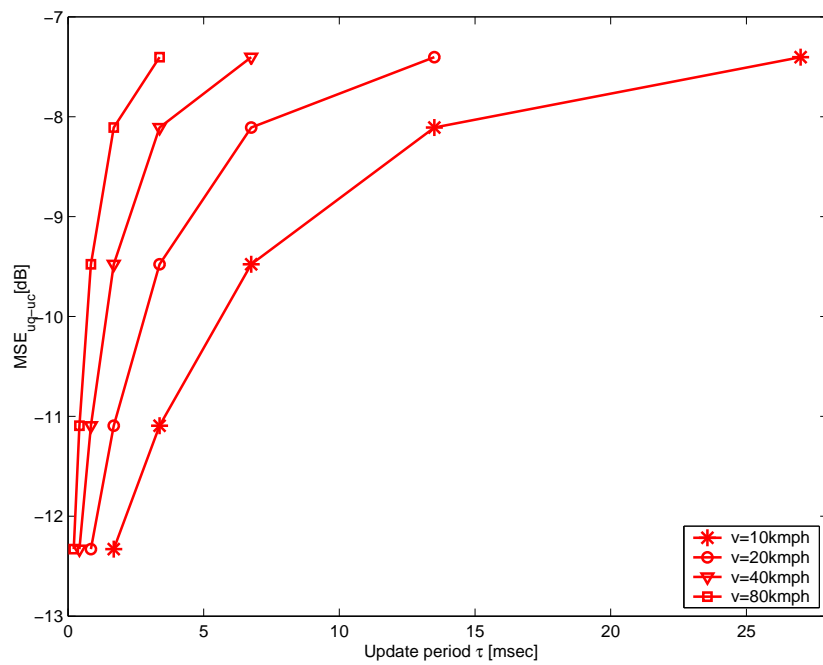


Figure 4.5: MSE vs. CSI update period, linear receiver, $f_c = 2\text{GHz}$, different mobile terminal velocities 10, 20, 40, 80kmph, average $SNR_{ul}^{csi} = 10\text{dB}$.

4.4 Case Study: UQ-UC CSI Feedback for Transmitter Optimization in Multiple Antenna Multiuser Systems

The discussion thus far has focused on performance limits and enhancements from the point of view of the MSE distortion achieved due to the UQ-UC CSI feedback transmission. A more direct performance issue that needs to be considered is the overall capacity of a system that actually uses the CSI feedback information. We will consider the UQ-UC CSI feedback in a multiple antenna multiuser system. As an example (previously presented in Chapter 3), consider the system shown in Figure 4.6, where there are M transmit antennas at the base station and N single-antenna mobile terminals. In the above model, x_n is the information bearing signal intended for mobile terminal n and y_n is the received signal at the corresponding terminal (for $n = 1, \dots, N$). The received vector $\mathbf{y} = [y_1, \dots, y_N]^T$ is

$$\begin{aligned} \mathbf{y} &= \mathbf{H}\mathbf{S}\mathbf{x} + \mathbf{n}, \\ \mathbf{y} &\in \mathcal{C}^N, \mathbf{x} \in \mathcal{C}^N, \mathbf{n} \in \mathcal{C}^N, \mathbf{S} \in \mathcal{C}^{M \times N}, \mathbf{H} \in \mathcal{C}^{N \times M} \end{aligned} \quad (4.20)$$

where $\mathbf{x} = [x_1, \dots, x_N]^T$ is the transmitted vector ($E[\mathbf{x}\mathbf{x}^H] = P_{dl} \mathbf{I}_{N \times N}$), \mathbf{n} is AWGN ($E[\mathbf{n}\mathbf{n}^H] = N_0 \mathbf{I}_{N \times N}$), \mathbf{H} is the MIMO channel response matrix, and \mathbf{S} is a transformation (spatial pre-filtering) performed at the transmitter. Note that the vectors \mathbf{x} and \mathbf{y} have the same dimensionality. Further, h_{nm} is the n th row and m th column element of the matrix \mathbf{H} corresponding to a channel between mobile terminal n and transmit antenna m .

Application of the spatial pre-filtering results in the composite MIMO channel \mathbf{G} given as

$$\mathbf{G} = \mathbf{H}\mathbf{S}, \quad \mathbf{G} \in \mathcal{C}^{N \times N} \quad (4.21)$$

where g_{nm} is the n th row and m th column element of the composite MIMO channel response matrix \mathbf{G} . The signal received at the n th mobile terminal is

$$y_n = \underbrace{g_{nn}x_n}_{\text{Desired signal for user } n} + \underbrace{\sum_{i=1, i \neq n}^N g_{ni}x_i}_{\text{Interference}} + n_n. \quad (4.22)$$

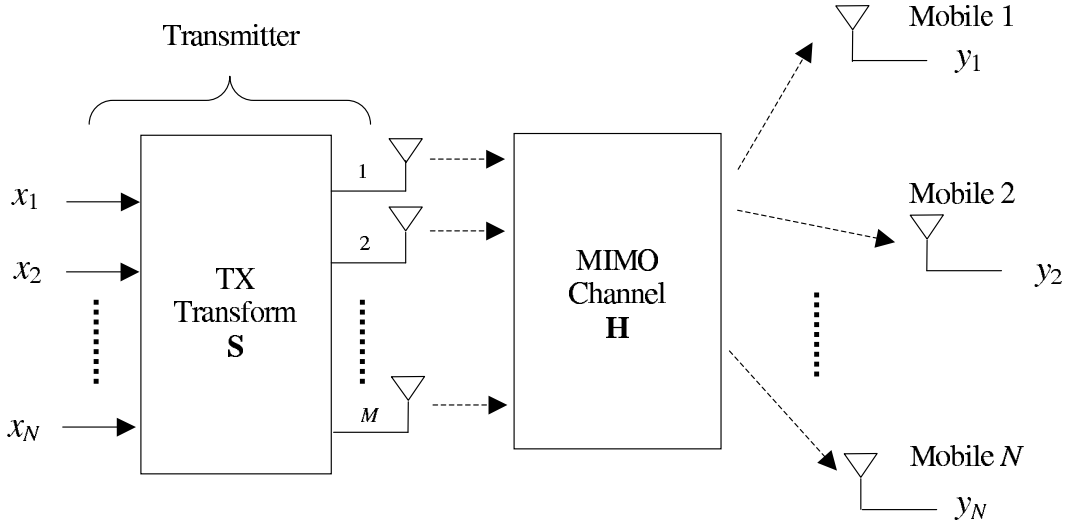


Figure 4.6: System model consisting of M transmit antennas and N mobile terminals.

In the above representation, the interference is the signal that is intended for other mobile terminals than terminal n . As said earlier, the matrix \mathbf{S} is a spatial pre-filter at the transmitter. It is determined based on optimization criteria that we address later in the text and has to satisfy the following constraint

$$\text{trace}(\mathbf{S}\mathbf{S}^H) \leq N \quad (4.23)$$

which keeps the average transmit power conserved. We represent the matrix \mathbf{S} as

$$\mathbf{S} = \mathbf{A}\mathbf{P}, \quad \mathbf{A} \in \mathcal{C}^{M \times N}, \mathbf{P} \in \mathcal{C}^{N \times N} \quad (4.24)$$

where \mathbf{A} is a linear transformation and \mathbf{P} is a diagonal matrix. \mathbf{P} is determined such that the transmit power remains conserved. We study the zero-forcing (ZF) spatial pre-filtering scheme where \mathbf{A} is represented by

$$\mathbf{A} = \mathbf{H}^H(\mathbf{H}\mathbf{H}^H)^{-1}. \quad (4.25)$$

As can be seen, the above linear transformation is zeroing the interference between the signals dedicated to different mobile terminals, i.e., $\mathbf{H}\mathbf{A} = \mathbf{I}_{N \times N}$. The x_n 's are assumed to be circularly symmetric complex random variables each having Gaussian distribution $\mathcal{N}_{\mathcal{C}}(0, P_{dl})$. Consequently, the maximum achievable data rate (capacity) for mobile terminal n is

$$R_n^{\text{ZF}} = \log_2 \left(1 + \frac{P_{dl}|p_{nn}|^2}{N_0} \right) \quad (4.26)$$

where p_{nn} is the n th diagonal element of the matrix \mathbf{P} defined in (4.24). The elements of the matrix \mathbf{P} are selected such that

$$\text{diag}(\mathbf{P}) = [p_{11}, \dots, p_{NN}]^T = \arg \max_{\text{trace}(\mathbf{A}\mathbf{P}\mathbf{P}^H\mathbf{A}^H) \leq N} \sum_{i=1}^N R_n. \quad (4.27)$$

For more details on the spatial pre-filtering, see Chapter 3 and [40, 72].

To perform the above spatial pre-filtering, the base station obtains CSI corresponding to each downlink channel state h_{nm} . The CSI is obtained from each mobile terminal using the UQ-UC CSI feedback. In other words, at time instant i , terminal n ($n = 1, \dots, N$) is transmitting the corresponding CSI $h_{nm}(i)$ ($m = 1, \dots, M$) via the uplink CSI feedback channel. Relating to the analysis in the previous sections, each $h_{nm}(i)$ corresponds to a different $h_{dl}(i)$. Instead of the ideal channel state $h_{nm}(i)$, the spatial pre-filter applies the estimate $\hat{h}_{nm}(i)$ obtained from the uplink CSI feedback receiver.

4.4.1 Numerical Results: Information Rates in Multiuser Systems

In Figure 4.7 we present downlink sum data rates for the downlink data, where $SNR_{dl} = 10 \log(P_{dl}/N_o) = 10 \text{dB}$, and $M = 3$ and $N = 3$. The rates are presented as functions of the mobile terminal velocity using the approximate the Jakes model for carrier frequency 2GHz and the CSI update period $\tau = 2 \text{msec}$ and spatially uncorrelated channels. Furthermore, the uplink CSI feedback channel is assumed to be *iid* Rayleigh with the average $SNR_{ul}^{csi} = 10 \text{dB}$. In addition, we present the rates for instantaneous ideal channel knowledge and a delayed ideal channel knowledge (2msec delay) which may correspond to a practical feedback scheme that quantizes and encodes the CSI. We note that under the UQ-UC CSI feedback with the linear receiver, the performance is better for channels with higher correlations (i.e., lower mobile terminal velocities). For the given update period $\tau = 2 \text{msec}$ and moderate and higher velocities, the UQ-UC CSI feedback scheme is outperforming the case of the delayed ideal channel knowledge.

In the above illustration, we have only considered the effect of temporal correlations

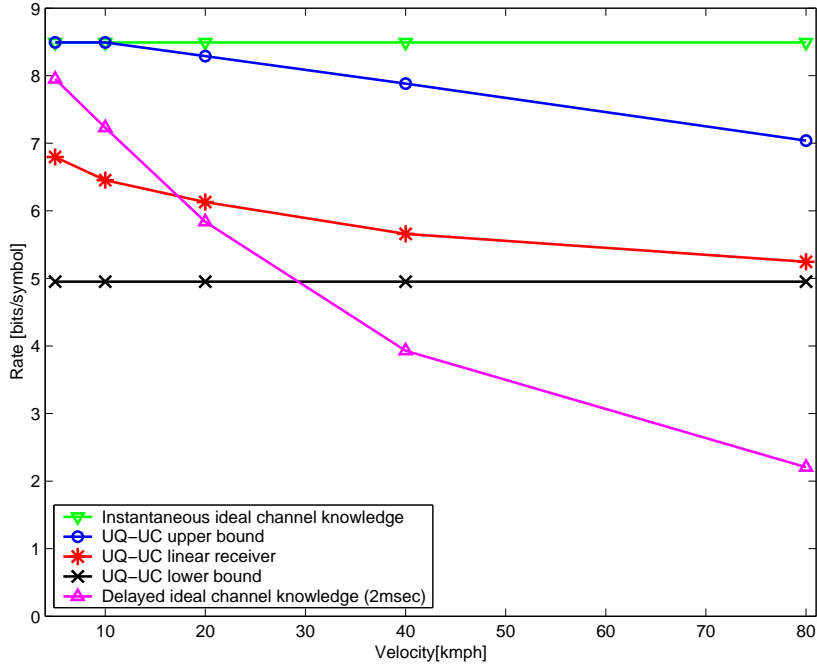


Figure 4.7: Average downlink sum data rate vs. the mobile terminal velocity, for CSI update period $\tau = 2\text{msec}$, $f_c = 2\text{GHz}$, $M = 3$, $N = 3$, spatially uncorrelated, downlink data $SNR_{dl} = 10\text{dB}$ and uplink CSI feedback $SNR_{ul}^{csi} = 10\text{dB}$.

in the downlink. Recent work on multiple antenna systems has revealed the importance of spatial correlations [63, 65–67] that can also significantly affect transmitter optimization schemes [72].

4.5 Conclusion

In this chapter we have considered a system where a mobile terminal obtains the downlink CSI and feeds it back to the base station using an uplink feedback channel. If the downlink channel is an independent Rayleigh fading channel, then the CSI may be viewed as an output of a complex independent identically distributed Gaussian source. Further, if the uplink feedback channel is AWGN, we have shown that unquantized and uncoded CSI transmission (that incurs zero delay) is optimal in that it achieves the same minimum mean squared error distortion as a scheme that optimally quantizes and encodes the CSI while incurring infinite delay. Furthermore, we presented the zero-delay UQ-UC CSI feedback scheme on correlated wireless channels. Since the UQ-UC

transmission is suboptimal in this case, we have proposed a simple linear CSI feedback receiver that exploits the correlations while still retaining the attractive zero-delay feature. Furthermore, we described the ARMA correlated channel model and presented the corresponding performance bounds for the UQ-UC CSI feedback scheme. We have shown that the linear receiver exploits the temporal correlations in the channel, resulting in lower MSE values when either the mobile terminal velocities are low or the CSI update period is small. We explored the performance limits of the scheme in the context of downlink multiple antenna, multiuser transmitter optimization.

Chapter 5

Conclusion

In this thesis we have studied the fundamental limits of multiple antenna multiuser systems in the following contexts: (1) pilot-assisted channel state estimation, (2) transmitter optimization with delayed CSI and (3) CSI feedback schemes.

We first have studied how the estimation error of the frequency-flat time-varying channel response affects the performance of a MIMO communication system. Using a block-fading channel model, we have connected results of information theory with practical pilot estimation for such systems. The presented analysis may be viewed as a study of mismatched receiver and transmitter algorithms in MIMO systems. We have considered two pilot based schemes for the estimation. The first scheme uses a single pilot symbol per block with different power than the data symbol power. The second scheme uses more than one pilot symbol per block, whose power is the same as the data symbol power. We have presented how the achievable data rates depend on the percentage of the total power allocated to the pilot, background noise level and the channel coherence time length. Our results have shown that the first pilot-based approach is less sensitive to the fraction of power allocated to the pilot. Furthermore, we have observed that as the number of transmit antennas increase, the sensitivity to the channel response estimation error is more pronounced (while keeping the same number of receive antennas). The effects of the estimation error are evaluated in the case of the estimates being available at the receiver only (open loop), and in the case when the estimates are fed back to the transmitter (closed loop) allowing water pouring transmitter optimization. In the case of water pouring transmitter optimization and the corresponding rates, we have not observed significant gains versus the open loop rates for the channel models considered here. Further, we observe that in certain cases,

it is better to use the open loop scheme as opposed to the closed loop scheme. The analysis presented here can be used to optimally allocate pilot power for various system and channel operating conditions, and to also determine the effectiveness of closed loop feedback.

Next, we have presented a study on multiple antenna transmitter optimization schemes that are based on linear transformations and transmit power optimization. We have shown that the triangularization with DPC approaches the closed loop MIMO rates (upper bound) for higher SNR. Further, the MZF solution performs very well for lower SNRs (approaching CL-MIMO and DPC rates), while for higher SNRs the rates for the ZF scheme converge to the MZF rates. In addition, we have shown how the average rates depend on number of transmit antennas, while keeping the number of terminals constant. With the number of transmit antennas increasing the rates increase, and the difference between the rates for different schemes gets smaller. Further, we have studied the performance of the transmitter optimization schemes with respect to the delayed CSI. It was seen that as the CSI delay increases, spatially uncorrelated channels perform worse than spatially correlated channels, which is in contrast to the case of zero delay CSI. A linear MMSE predictor of the channel state was also introduced which improved the performance in all cases. Further, we have shown that the predictor increases the tolerable maximum CSI delay for which the performance on spatially uncorrelated channels exceeds that of the correlated case. The results have suggested that the temporal correlations in the channel alone are significant enough to support the application of the MMSE prediction.

Finally, we have considered a system where a mobile terminal obtains the downlink CSI and feeds it back to the base station using an uplink feedback channel. If the downlink channel is an independent Rayleigh fading channel, then the CSI may be viewed as an output of a complex independent identically distributed Gaussian source. Further, if the uplink feedback channel is AWGN, we have shown that unquantized and uncoded CSI transmission (that incurs zero delay) is optimal in that it achieves the same minimum mean squared error distortion as a scheme that optimally quantizes and encodes the CSI while incurring infinite delay. Furthermore, we presented the

zero-delay UQ-UC CSI feedback scheme on correlated wireless channels. Since the UQ-UC transmission is suboptimal in this case, we have proposed a simple linear CSI feedback receiver that exploits the correlations while still retaining the attractive zero-delay feature. Furthermore, we described the ARMA correlated channel model and presented the corresponding performance bounds for the UQ-UC CSI feedback scheme. We have shown that the linear receiver exploits the temporal correlations in the channel, resulting in lower MSE values when either the mobile terminal velocities are low or the CSI update period is small. We explored the performance limits of the scheme in the context of downlink multiple antenna multiuser transmitter optimization.

5.1 Future Directions

In this section we briefly outline potential future topics that are extensions of the work presented in this thesis.

Considering the pilot-assisted channel state estimation (in Chapter 2), the following topics seem promising.

1. Motivated by the achievable data rates in the case of zero pilot power (e.g., see results in Figure 2.3), analysis and design of differential transmission schemes appears to be of interest. Furthermore, considering the importance of the low SNR regime and/or very high mobility, understanding performance limits of ON/OFF keying and its comparison to pilot-assisted or differential schemes may be a topic of future study.
2. The independent block fading channel model could be extended to more realistic temporally and spatially correlated channel models that are, for example, presented in Chapter 3. Understanding its implication on open loop (in particular the aspect of continuous channel variations) and closed loop (in particular the aspect of temporal and spatial correlations) systems could be of interest.

Regarding the transmitter optimization with delayed CSI (in Chapter 3), the following topics may be of interest.

1. TDD uplink/downlink multiplexing directly allows the transmitter to obtain the CSI. Consequently, an analysis of TDD wireless systems is needed. In particular, joint channel response estimation for multiple uplink asynchronous transmission may be a topic of future studies.
2. Environments that offer narrow angular spread should be considered because they may allow a base station to obtain downlink CSI without explicit feedback from a mobile terminal (estimating a partial downlink CSI based on the uplink CSI). This scenario is of particular importance in FDD cellular systems [73] and it deserves further study.
3. Further analysis and improvements of the channel state prediction schemes are needed. For example, their validation using real propagation measurements may be of interest.

We believe that the presented study on the UQ-UC CSI feedback scheme (in Chapter 4) offers a number of research topics. In the following we list just a few.

1. Motivated by the performance bounds presented in Chapter 4, future work could result in CSI feedback schemes that further approach them.
2. There is a need for understanding the trade-off between resources (e.g., power, time and spectrum) allocated to the pilots and the CSI feedback versus the resources of the data carrying signals on the downlink and uplink. For example, having more resources allocated to the pilots and the CSI feedback reduces the distortion of the CSI at the base station. However, since the resources are finite, this correspondingly lowers the resources available for the data carrying signals (lowering the uplink and downlink rate). Due to these opposing trends, how to optimize the resource allocation may be a subject of further studies.
3. Another future issue of interest is to compare the presented UQ-UC CSI feedback scheme to different schemes that use quantization (i.e., source coding) and channel coding optimized for a given delay constraint.

Chapter A

Virtual Uplink and Proof of Proposition 2

Let us describe the corresponding virtual uplink for the system in Figure 3.1. Let \bar{x}_n be the uplink information bearing signal transmitted from mobile terminal n ($n = 1, \dots, N$) and \bar{y}_m be the received signal at the m th base station antenna ($m = 1, \dots, M$). \bar{x}_n are assumed to be circularly symmetric complex random variables having Gaussian distribution $\mathcal{N}_{\mathcal{C}}(0, P_{av})$. Further, the received vector $\bar{\mathbf{y}} = [\bar{y}_1, \dots, \bar{y}_M]^T$ is

$$\begin{aligned}\bar{\mathbf{y}} &= \bar{\mathbf{H}}\bar{\mathbf{x}} + \bar{\mathbf{n}} = \mathbf{H}^H\bar{\mathbf{x}} + \bar{\mathbf{n}}, \\ \bar{\mathbf{y}} &\in \mathcal{C}^M, \bar{\mathbf{x}} \in \mathcal{C}^N, \bar{\mathbf{n}} \in \mathcal{C}^M, \bar{\mathbf{H}} \in \mathcal{C}^{M \times N}\end{aligned}\tag{A.1}$$

where $\bar{\mathbf{x}} = [\bar{x}_1, \dots, \bar{x}_N]^T$ is the transmitted vector ($\mathbb{E}[\bar{\mathbf{x}}\bar{\mathbf{x}}^H] = P_{av} \mathbf{I}_{N \times N}$), $\bar{\mathbf{n}}$ is AWGN ($\mathbb{E}[\bar{\mathbf{n}}\bar{\mathbf{n}}^H] = N_0 \mathbf{I}_{M \times M}$) and $\bar{\mathbf{H}} = \mathbf{H}^H$ is the uplink MIMO channel response matrix.

It is well known that the MMSE receiver is the optimal linear receiver for the uplink (*multiple access channel*) [74, 75]. It maximizes the received SINR (and rate) for each user. The decision statistic is obtained after the receiver MMSE filtering as

$$\bar{\mathbf{x}}^{dec} = \mathbf{W}^H \bar{\mathbf{y}}\tag{A.2}$$

where the MMSE receiver is

$$\mathbf{W} = \left(\left(\mathbf{H}\mathbf{H}^H + \frac{N_0}{P_{av}} \mathbf{I} \right)^{-1} \mathbf{H} \right)^H = \mathbf{H}^H \left(\mathbf{H}\mathbf{H}^H + \frac{N_0}{P_{av}} \mathbf{I} \right)^{-1}.\tag{A.3}$$

Proof of Proposition 2

Note that $\mathbf{W} = \mathbf{A}$ in (3.8), for the MZF transmitter spatial pre-filtering. Let us normalize the column vectors of the matrix \mathbf{W} in (A.3) as

$$\mathbf{W}_{nor} = \mathbf{W}\mathbf{P}\tag{A.4}$$

where \mathbf{P} is defined in (3.10). In other words the n th diagonal element of \mathbf{P} is selected as

$$p_{nn} = \frac{1}{\sqrt{\mathbf{w}_n^H \mathbf{w}_n}} \quad (n = 1, \dots, N) \quad (\text{A.5})$$

where \mathbf{w}_n is the n th column vector of the matrix \mathbf{W} (where $\mathbf{w}_n = \mathbf{a}_n$, which is the column vector of \mathbf{A} for $n = 1, \dots, N$). It is well known that any normalization of the columns of the MMSE receiver in (A.3) does not change the SINRs. In other words, the SINR for the n th uplink user ($n = 1, \dots, N$) is

$$SINR_n^{UL} = \frac{P_{av} |\mathbf{w}_n^H \bar{\mathbf{h}}_n|^2}{P_{av} \sum_{i=1, i \neq n}^N |\mathbf{w}_n^H \bar{\mathbf{h}}_i|^2 + N_0 \mathbf{w}_n^H \mathbf{w}_n} = \frac{P_{av} |\mathbf{w}_n^H \bar{\mathbf{h}}_n|^2 / (\mathbf{w}_n^H \mathbf{w}_n)}{P_{av} \sum_{i=1, i \neq n}^N |\mathbf{w}_n^H \bar{\mathbf{h}}_i|^2 / (\mathbf{w}_n^H \mathbf{w}_n) + N_0} \quad (\text{A.6})$$

where $\bar{\mathbf{h}}_n$ is the n th column vector of the matrix $\bar{\mathbf{H}}$. Note that $\bar{\mathbf{h}}_n^H = \mathbf{h}_n$ which is the n th row vector of the downlink MIMO channel \mathbf{H} . The corresponding downlink SINR when the MZF spatial per-filtering is used (with \mathbf{P} defined in (3.10)) is

$$SINR_n^{MZF} = \frac{P_{av} |\mathbf{h}_n \mathbf{a}_n|^2 / (\mathbf{a}_n^H \mathbf{a}_n)}{P_{av} \sum_{i=1, i \neq n}^N |\mathbf{h}_i \mathbf{a}_i|^2 / (\mathbf{a}_n^H \mathbf{a}_n) + N_0}. \quad (\text{A.7})$$

As said earlier, $\mathbf{w}_n = \mathbf{a}_n$ and $\bar{\mathbf{h}}_n^H = \mathbf{h}_n$. Thus, $SINR_n^{MZF} = SINR_n^{UL}$ for $n = 1, \dots, N$ leading to identical rates which concludes the proof.

Chapter B

Dirty Paper Coding

One practical, but suboptimal single-dimensional DPC solution is described in [60, 61]. Starting from that solution we introduce the DPC scheme.

The transmitted signal in (3.1) intended for terminal n is

$$x_n = f_{mod}(\hat{x}_n - I_n) \quad (\text{B.1})$$

where \hat{x}_n is the information bearing signal for terminal n and $f_{mod}(\cdot)$ is a modulo operation (i.e., a uniform scalar quantizer). For a real variable x , $f_{mod}(x)$ is defined as

$$f_{mod}(x) = ((x + Z) \bmod (2Z)) - Z \quad (\text{B.2})$$

and in the case of a complex variable $a + jb$, $f_{mod}(a + jb) = f_{mod}(a) + jf_{mod}(b)$. The constant Z is selected such that $E[x_n x_n^*] = P_{av}$. Further, from (3.12), I_n is the normalized interference at terminal n

$$I_n = \sum_{i=1}^{n-1} g_{ni} x_i / g_{nn} \quad (\text{B.3})$$

assuming that $g_{nn} \neq 0$. Note that I_n is only known at the transmitter. At terminal n the following operation is performed

$$f_{mod}(y_n / g_{nn}) = \hat{x}_n + n_n^* \quad (\text{B.4})$$

where n_n^* is a wrapped-around AWGN (due to the nonlinear operation $f_{mod}(\cdot)$). For high SNR and with \hat{x}_n being uniformly distributed over the single-dimensional region, the achievable rate is approximately 1.53dB away from the rate in (3.13) [60, 61].

To further approach the rate in (3.13), based on [60], the following modifications of the suboptimal scheme in (B.1) are needed. The transmitted signal intended for terminal n is now

$$x_n = f_k(\hat{x}_n - \xi_n I_n + d_n) \quad (\text{B.5})$$

where $f_k(\cdot)$ is a modulo operation over a k -dimensional region. ξ_n is a parameter to be optimized ($0 < \xi_n \leq 1$) and d_n is a dither (uniformly distributed pseudo noise over the k -dimensional region). At terminal n the following operation is performed,

$$f_k(y_n/g_{nn}) = \hat{x}_n + (1 - \xi_n)u_n + \xi_n n_n^* \quad (\text{B.6})$$

where n_n^* is a wrapped-around AWGN (due to the nonlinear operation $f_k(\cdot)$) and u_n is uniformly distributed over the k -dimensional region. For $k \rightarrow \infty$ and \hat{x}_n being uniformly distributed over the k -dimensional region, the rate in (3.13) can be achieved [60]. Further details on selecting ξ_n and d_n are beyond the scope of this thesis. We refer the reader to [60] and references therein.

Chapter C

ARMA Model and Approximation of the Jakes Model

In this appendix we show how for the given correlation between the downlink channel states, the coefficients c_0 to c_L of the ARMA model in (4.9) are determined. The correlation between the downlink channel states is given as

$$\phi(k) = \mathbf{E}[h_{dl}(i)h_{dl}(i-k)^*] \text{ for } |k| \leq L \quad (\text{C.1})$$

where $\phi(-k) = \phi(k)^*$, and for $|k| > L$, $\phi(k) = 0$. Further, based on the ARMA model in (4.9) we form a set of $2L$ linear equations

$$\phi(0) = \sum_{j=1}^L c_j \phi(-j) + c_0^2 \quad (\text{C.2})$$

and

$$\phi(k) = \sum_{j=1}^L c_j \phi(k-j) \quad k = 1, \dots, 2L-1. \quad (\text{C.3})$$

Let us define the following matrix

$$\Phi = \begin{bmatrix} 1 & \phi(1)^* & \phi(2)^* & \cdots & \phi(L)^* \\ 0 & \phi(0) & \phi(1)^* & \cdots & \phi(L-1)^* \\ \vdots & \vdots & \vdots & & \vdots \\ 0 & \phi(L-1) & \phi(L-2) & \cdots & \phi(0) \\ 0 & 0 & \phi(L-1) & \cdots & \phi(1) \\ \vdots & \vdots & \vdots & & \vdots \\ 0 & 0 & 0 & \cdots & \phi(L-1) \end{bmatrix} \quad (\text{C.4})$$

and vectors

$$\mathbf{c} = [c_0^2 \ c_1 \ \cdots \ c_L]^T \quad (\text{C.5})$$

and

$$\mathbf{f} = [\phi(0) \ \phi(1) \ \cdots \ \phi(L) \ \underbrace{0 \ \cdots \ 0}_{L-1}]^T. \quad (\text{C.6})$$

The above system of linear equations can be rewritten as

$$\mathbf{f} = \Phi \mathbf{c}. \quad (\text{C.7})$$

By construction, the columns of the matrix Φ are linearly independent. Thus, the least squares solution of the above linear equation is

$$\tilde{\mathbf{c}} = (\Phi^H \Phi)^{-1} \Phi^H \mathbf{f}. \quad (\text{C.8})$$

With $c_0 \geq 0$, the above solution determines the coefficients c_0 to c_L of the ARMA model in (4.9).

To approximate the Jakes model using the finite length ARMA model in (4.9) we select elements of the vector \mathbf{f} as

$$\phi(k) = J_0(2\pi f_d k \tau), \quad k = 0, \dots, L \quad (\text{C.9})$$

where f_d is the maximum Doppler frequency and τ is the time difference between successive channel states $h_{dl}(i)$ and $h_{dl}(i-1)$. Satisfying the Nyquist sampling rate the update period τ should be such that

$$\tau < \frac{1}{2f_d}. \quad (\text{C.10})$$

Specifically, in the case of the numerical results in Chapter 4 the length L is selected as

$$L \geq \frac{4}{\tau f_d}. \quad (\text{C.11})$$

References

- [1] G. J. Foschini, "Layered space-time architecture for wireless communication in a fading environment when using multiple antennas," *Bell Labs Technical Journal*, vol. 1, no. 2, pp. 41–59, 1996.
- [2] G. J. Foschini and M. J. Gans, "On limits of wireless communications in a fading environment when using multiple antennas," *Wireless Personal Communications*, no. 6, pp. 315–335, 1998.
- [3] D. Chizhik, G. J. Foschini, M. J. Gans, and R. Valenzuela, "Keyholes, correlations, and capacities of multielement transmit and receive antennas," *IEEE Transactions on Wireless Communications*, vol. 1, pp. 361–368, April 2002.
- [4] D. Chizhik, J. Ling, P. W. Wolniansky, R. A. Valenzuela, N. Costa, and K. Huber, "Multiple input multiple output measurements and modeling in Manhattan," *VTC Fall*, vol. 1, pp. 107–110, 2002.
- [5] P. Soma, D. S. Baum, V. Erceg, R. Krishnamoorthy, and A. Paulraj, "Analysis and modeling of multiple-input multiple-output (MIMO) radio channel based on outdoor measurements conducted at 2.5 GHz for fixed BWA applications," *IEEE Conference ICC 2002*, pp. 272–276, 2002.
- [6] G. J. Foschini, G. D. Golden, R. A. Valenzuela, and P. W. Wolniansky, "Simplified processing for wireless communications at high spectral efficiency," *IEEE JSAC*, vol. 17, pp. 1841–1852, November 1999.
- [7] J. C. Guey, M. P. Fitz, M. R. Bell, and W. Y. Kuo, "Signal design for transmitter diversity wireless communication systems over Rayleigh fading channels," *IEEE Transactions on Communications*, vol. 47, pp. 527–537, 1999.
- [8] D. Samardzija, P. Wolniansky, and J. Ling, "Performance evaluation of the VBLAST algorithm in W-CDMA systems," *The IEEE Vehicular Technology Conference (VTC)*, vol. 2, pp. 723–727, September 2001. Atlantic City.
- [9] D. Guo and X. Wang, "Blind detection in MIMO systems via sequential Monte Carlo," *IEEE JSAC*, vol. 21, pp. 464–473, April 2003.
- [10] A. Gorokhov, D. Gore, and A. Paulraj, "Receive antenna selection for MIMO flat-fading channels: theory and algorithms," *IEEE Transactions on Information Theory*, vol. 49, pp. 2687–2696, October 2003.
- [11] Z. Hong, K. Liu, R. W. Heath, and A. M. Sayeed, "Spatial multiplexing in correlated fading via the virtual channel representation," *IEEE JSAC*, vol. 21, pp. 856–866, June 2003.

- [12] M. Kang and M. Alouini, "Largest eigenvalue of complex Wishart matrices and performance analysis of MIMO MRC systems," *IEEE JSAC*, vol. 21, pp. 418–426, April 2003.
- [13] A. F. Molisch, M. Z. Win, and J. H. Winters, "Reduced complexity transmit-receive diversity systems," *IEEE Transactions on Signal Processing, Special Issue on MIMO*, vol. 51, pp. 2729–2738, November 2003.
- [14] B. Dong, X. Wang, and A. Doucet, "A new class of soft MIMO demodulation algorithms," *IEEE Transactions on Signal Processing, Special Issue on MIMO*, vol. 51, pp. 2752–2763, November 2003.
- [15] J. M. Kim and V. Tarokh, "Variable rate space-time block codes in M-ary PSK systems," *IEEE JSAC*, vol. 21, pp. 362–373, April 2003.
- [16] M. J. Borran, A. Sabharwal, and B. Aazhang, "On design criteria and construction of noncoherent space-time constellations," *IEEE Transactions on Information Theory*, vol. 49, pp. 2332–2351, October 2003.
- [17] M. O. Damen, H. El Gamal, and N. C. Beaulieu, "Linear threaded algebraic space-time constellations," *IEEE Transactions on Information Theory*, vol. 49, pp. 2372–2388, October 2003.
- [18] Y. Jing and B. Hassibi, "Unitary space-time modulation via the Cayley transform," *IEEE Transactions on Signal Processing, Special Issue on MIMO*, vol. 51, pp. 2891–2904, November 2003.
- [19] A. Matache and R. D. Wesel, "Universal trellis codes for diagonally layered space-time systems," *IEEE Transactions on Signal Processing, Special Issue on MIMO*, vol. 51, pp. 2773–2783, November 2003.
- [20] M. K. Simon and H. Jaffarkhani, "Performance evaluation of super-orthogonal space-time trellis codes using a moment generating function-based approach," *IEEE Transactions on Signal Processing, Special Issue on MIMO*, vol. 51, pp. 2773–2783, November 2003.
- [21] G. D. Golden, G. J. Foschini, R. A. Valenzuela, and P. W. Wolniansky, "Detection algorithm and initial laboratory results using V-BLAST space-time communication architecture," *Electronics Letters*, vol. 35, pp. 14–16, January 1999.
- [22] H. Zheng and D. Samardzija, "Performance evaluation of indoor wireless system using BLAST testbed," *The IEEE Vehicular Technology Conference (VTC)*, vol. 2, pp. 905–909, October 2001. Atlantic City.
- [23] D. Samardzija, C. Papadias, and R. A. Valenzuela, "Experimental evaluation of unsupervised channel deconvolution for wireless multiple-transmitter/multiple-receiver systems," *Electronic Letters*, pp. 1214–1215, September 2002.
- [24] S. Lang, R. M. Rao, and B. Daneshrad, "Design and development of a 5.25GHz software defined wireless OFDM communication platform," *IEEE Communications Magazine*, 2004. Submitted.

- [25] G. Caire and S. Shamai, "On the achievable throughput of a multiantenna Gaussian broadcast channel," *IEEE Transactions on Information Theory*, vol. 49, pp. 1691–1706, July 2003.
- [26] D. Tse and P. Viswanath, "On the capacity region of the vector Gaussian broadcast channel," *IEEE International Symposium on Information Theory*, pp. 342–342, July 2003.
- [27] S. Vishwanath, G. Kramer, S. Shamai, S. Jafar, and A. Goldsmith, "Capacity bounds for Gaussian vector broadcast channel," *The DIMACS Workshop on Signal Processing for Wireless Transmission*, vol. 62, pp. 107–122, October 2002. Rutgers University.
- [28] R. S. Blum, "MIMO capacity with interference," *IEEE JSAC*, vol. 21, pp. 793–801, June 2003.
- [29] S. Ye and R. S. Blum, "Optimized signaling for MIMO interference systems with feedback," *IEEE Transactions on Signal Processing, Special Issue on MIMO*, vol. 51, pp. 2839–2848, November 2003.
- [30] W. Rhee and J. M. Cioffi, "On the capacity of multiuser wireless channels with multiple antennas," *IEEE Transactions on Information Theory*, vol. 49, pp. 2580–2595, October 2003.
- [31] J. N. Laneman and G. W. Wornell, "Distributed space-time coding protocols for exploiting cooperative diversity in wireless networks," *IEEE Transactions on Information Theory*, vol. 49, pp. 2415–2425, October 2003.
- [32] E. Rashid-Farrohi, L. Tassiulas, and K. Liu, "Joint optimal power control and beamforming in wireless networks using antenna arrays," *IEEE Transactions on Communications*, vol. 46, pp. 1313–1323, October 1998.
- [33] E. Visotsky and U. Madhow, "Optimum beamforming using transmit antenna arrays," *The IEEE Vehicular Technology Conference (VTC)*, vol. 1, pp. 851–856, May 1999.
- [34] A. Lapidoth and S. Shamai, "Fading channels: how perfect need "perfect side information" be?," *IEEE Transaction on Information Theory*, vol. 48, pp. 1118–1134, May 2002.
- [35] S. Shamai and T. Marzetta, "Multiuser capacity in block fading with no channel state information," *IEEE Transaction on Information Theory*, vol. 48, pp. 938–942, April 2002.
- [36] T. L. Marzetta, "Blast training: estimating channel characteristics for high-capacity space-time wireless," *37th Annual Allerton Conference on Communications, Control and Computing*, September 1999.
- [37] J. Baltersee, G. Fock, and H. Meyr, "Achievable rate of MIMO channels with data-aided channel estimation and perfect interleaving," *IEEE JSAC*, vol. 19, pp. 2358–2368, December 2001.

- [38] B. Hassibi and B. M. Hochwald, "How much training is needed in multiple-antenna wireless links," *Technical Memorandum, Bell Laboratories, Lucent Technologies*, October 2001.
- [39] D. Samardzija and N. Mandayam, "Pilot assisted estimation of MIMO fading channel response and achievable data rates," *IEEE Transactions on Signal Processing, Special Issue on MIMO*, vol. 51, pp. 2882–2890, November 2003.
- [40] D. Samardzija and N. Mandayam, "Multiple antenna transmitter optimization schemes for multiuser systems," *The IEEE Vehicular Technology Conference (VTC)*, October 2003. Orlando.
- [41] D. Samardzija and N. Mandayam, "Pilot assisted estimation of MIMO fading channel response and achievable data rates," *The DIMACS Workshop on Signal Processing for Wireless Transmission*, vol. 62, pp. 255–270, October 2002. Rutgers University.
- [42] D. Samardzija and N. Mandayam, "Unquantized and uncoded channel state information feedback on wireless channels," *Conference on Information Sciences and Systems*, March 2004. Princeton University.
- [43] E. Biglieri, J. Proakis, and S. Shamai, "Fading channels: information-theoretic and communications aspects," *IEEE Transactions on Information Theory*, vol. 44, pp. 2619–2692, October 1998.
- [44] G. L. Stuber, *Principles of Mobile Communications*. Kluwer Academic Publishers, first ed., 1996.
- [45] H. V. Poor, *An Introduction to Signal Detection and Estimation*. Springer-Verlag, second ed., 1994.
- [46] H. Holma and A. Toskala, eds., *WCDMA for UMTS*. Wiley, first ed., 2000.
- [47] A. Burg, E. Beck, D. Samardzija, M. Rupp, and et al., "Prototype experience for MIMO BLAST over third generation wireless system," *IEEE JSAC Special Issue on MIMO Systems and Applications*, vol. 21, pp. 440–451, April 2003.
- [48] J. C. Guey, M. P. Fitz, M. R. Bell, and W. Kuo., "Signal design for transmitter diversity wireless communication systems over Rayleigh fading channels," *Proc. of IEEE Vehicular Technology Conference*, vol. 1, pp. 136–140, 1996. Atlanta.
- [49] D. Shiu, G. J. Foschini, and M. J. Gans, "Fading correlation and its effects on the capacity of multielement antenna systems," *IEEE Transactions on Communications*, vol. 48, pp. 502–513, March 2000.
- [50] J. G. Proakis, *Digital Communications*. New York: McGraw-Hill, 3rd ed., 1995.
- [51] L. Li and A. Goldsmith, "Capacity and optimal resource allocation for fading broadcast channels - part I: ergodic capacity," *IEEE Transactions on Information Theory*, vol. 47, pp. 1083–1102, March 2001.
- [52] J. M. Wozencraft and I. M. Jacobs, *Principles of Communication Engineering*. New York: Wiley, 1965.

- [53] R. G. Gallager, *Information Theory and Reliable Communications*. New York: John Wiley and Sons, 1968.
- [54] A. Goldsmith and P. Varaiya, "Increasing spectral efficiency through power control," *ICC*, vol. 1, pp. 600–604, 1993.
- [55] G. Strang, *Linear Algebra and Its Applications*. Harcourt Brace Jovanovich, third ed., 1988.
- [56] C. Wen, Y. Wang, and J. Chen, "Adaptive spatio-temporal coding scheme for indoor wireless communication," *IEEE JSAC*, vol. 21, pp. 161–170, February 2003.
- [57] T. M. Cover and J. A. Thomas, *Elements of Information Theory*. Wiley Publications, first ed., 1991.
- [58] E. Visotsky and U. Madhow, "Space-time transmit precoding with imperfect feedback," *IEEE Transactions on Information Theory*, vol. 47, pp. 2632–2639, September 2001.
- [59] M. H. M. Costa, "Writing on dirty paper," *IEEE Transactions on Information Theory*, vol. 29, pp. 439–441, May 1983.
- [60] G. J. Foschini and A. H. Diaz, "Dirty paper coding: perturbing off the infinite dimensional lattice limit," *The DIMACS Workshop on Signal Processing for Wireless Transmission*, vol. 62, pp. 141–160, October 2002. Rutgers University.
- [61] U. Erez, R. Zamir, and S. Shamai, "Additive noise channels with side information at the transmitter," *The 21st IEEE Convention of the Electrical and Electronic Engineers in Israel*, pp. 373–376, April 2000.
- [62] A. S. Cohen and A. Lapidoth, "Generalized writing on dirty paper," *IEEE International Symposium on Information Theory*, p. 227, 2002.
- [63] K. Pedersen, P. Mogensen, and B. Fleury, "A stochastic model of the temporal and azimuthal dispersion seen at the base station in outdoor propagation environments," *IEEE Transactions on Vehicular Technology*, vol. 49, pp. 437–447, March 2000.
- [64] T. Chu and L. J. Greenstein, "A semi-empirical representation of antenna diversity gain at cellular and PCS base stations," *IEEE Transactions on Communications*, vol. 45, pp. 644–646, June 1997.
- [65] Q. Spencer, B. Jeffs, M. Jensen, and A. Swindlehurst, "Modeling the statistical time and angle of arrival characteristics of an indoor multipath channel," *IEEE Journal on Selected Areas in Communications*, vol. 18, pp. 347–360, March 2000.
- [66] H. Xu, D. Chizhik, H. Huang, and R. Valenzuela, "A wave-based wideband MIMO channel modeling technique," *Personal, Indoor and Mobile Radio Communications*, vol. 4, pp. 1626–1630, September 2002.
- [67] D. Chizhik, "Slowing the time-fluctuating MIMO channel by beam-forming," *To appear in IEEE Transactions on Wireless Communications*.

- [68] S. Haykin, *Adaptive Filter Theory*. Prentice-Hall, second ed., 1991.
- [69] T. J. Goblick, "Theoretical limitations on the transmission of data from analog sources," *IEEE Transactions on Information Theory*, vol. 11, pp. 558–567, October 1965.
- [70] T. Berger, "Shannon lecture: living information theory," *Presented at IEEE ISIT*, July 2002.
- [71] M. Gastpar, B. Rimoldi, and M. Vetterli, "To code, or not to code: lossy source channel communication revisited," *IEEE Transactions on Information Theory*, vol. 49, pp. 1147–1158, May 2003.
- [72] D. Samardzija and N. Mandayam, "Downlink multiple antenna transmitter optimization on spatially and temporally correlated channels with delayed channel state information," *Conference on Information Sciences and Systems*, March 2004. Princeton University.
- [73] K. Pedersen, P. Mogensen, and J. Ramiro-Moreno, "Application and performance of downlink beamforming techniques in UMTS," *IEEE Communications Magazine*, pp. 134–143, October 2003.
- [74] U. Madhow and M. Honig, "MMSE interference suppression for direct-sequence spread-spectrum CDMA," *IEEE Transactions on Communications*, vol. 42, pp. 3178–3188, December 1994.
- [75] S. Verdú, *Multiuser Detection*. Cambridge University Press, 1998.

Vita

Dragan Samardzija

- 1972, March 1 Born in, Kikinda, Serbia.
- 1991-1996 Attended the University of Novi Sad, Yugoslavia. Received the B.S. degree in electrical engineering and computer science in 1996.
- 1999-2000 Attended the Graduate School - New Brunswick, Rutgers, the State University of New Jersey. Research assistant at Wireless Information Network Laboratory (WINLAB), department of electrical and computer engineering. Received the M.S. degree in electrical engineering in 2000.
- 2000-present A member of technical staff at the Wireless Research Laboratory, Bell Laboratories, Lucent Technologies. Involved in research in the field of MIMO wireless systems. His research interests include detection, estimation, information theory and implementation aspects of MIMO and multiple-access wireless systems. As a member of the BLAST project team, a recipient of the 2002 Bell Laboratories President's Award.

Publications

1. D. Samardzija, N. Mandayam "Pilot assisted estimation of MIMO fading channel response and achievable data rates," *IEEE Transactions on Signal Processing, Special Issue on MIMO*, vol. 51, pp. 2882-2890, November 2003.
2. A. Burg, E. Beck, D. Samardzija, M. Rupp, et al., "Prototype experience for MIMO BLAST over third generation wireless system," *IEEE JSAC on MIMO Systems and Applications: Part I*, vol. 21, pp. 440-451, April 2003.
3. D. Samardzija, C. Papadias, R. Valenzuela, "Experimental evaluation of unsupervised channel deconvolution for wireless multiple-transmitter/multiple-receiver systems," *Electronics Letters IEE*, September 2002.
4. D. Samardzija, N. Mandayam, I. Seskar, "Blind successive interference cancellation for DS-CDMA systems," *IEEE Transactions on Communications*, vol. 50, pp. 276-290, February 2002.
5. D. Samardzija, N. Mandayam, I. Seskar, "Multistage nonlinear blind interference cancellation for DS-CDMA systems," *Journal of VLSI Signal Processing* 30, pp. 257-271, 2002 Kluwer Academic Press.